UNITED NATIONS EDUCATIONAL, SCIENTIFIC AND CULTURAL ORGANIZATION
INTERNATIONAL ATOMIC ENERGY AGENCY
INTERNATIONAL CENTRE FOR THEORETICAL PHYSICS
I.C.T.P., P.O. BOX 586, 34100 TRIESTE, ITALY, CABLE: CENTRATOM TRIESTE

SMR.961 - 12

WORKSHOP ON:
PROTEINS, MEMBRANES and their INTERACTIONS

22 JULY - 2 AUGUST 1996

"Membrane-proteins: structure and interactions" Part I

"Lamellar biogels: fluid membrane hydrogels containing polymer-lipids" Part II

"DNA interactions with cationic membranes" Part III

Cyrus SAFINYA
University of California at Santa Barbara
Department of Physics
CA 93106-9530 Santa Barbara
U.S.A.

Biomaterials
Editorial overview

Cyrus R Safinya* and Lia Addadi†

Addresses
*Materials Research Laboratory, Materials Department, Physics Department, and Biochemistry and Molecular Biology Program, University of California, Santa Barbara, CA 93106, USA; e-mail: safinya@engineering.ucsb.edu
†Department of Structural Biology, Weizmann Institute of Science, Rehovot 76100, Israel; e-mail: csaddadi@weizmann.weizmann.ac.il

Current Opinion in Solid State & Materials Science 1996, 1:387–391

 ISSN 1359-0286

Biomolecular materials and engineering

Biomolecular materials are materials that result from research at the interface between materials science and engineering and biology [1]. This highly interdisciplinary research enterprise claims practitioners from diverse disciplines, including soft condensed matter physics, complex fluids, biophysics, chemical synthesis, biochemistry, molecular cell biology and genetic engineering. In most cases a common structural feature of such materials is self-assembly, in particular, into higher-ordered supramolecular materials.

Among the most interesting biomolecular materials are those made up of self-assembled and functionalized interfaces where the fuctionality is derived from biomolecules which may be manipulated at the molecular level. For example, two-dimensional self-assemblies of membrane-proteins, such as bacteriorhodopsin and similar native bacterial self-assemblies of surface protein layers, are of current interest for the development of biomolecular materials in technological areas as diverse as molecular electronics and optical switch applications [2], to uses as molecular sieves [3,4] and the lithographic fabrication of nanometer scale patterns [5]. Functionalized biomolecular interfaces which include receptor proteins, could form the basis for developing advanced materials that serve as chemical and biological sensors [6], or those with controlled interfacial properties such as adhesion and lubrication [7]. In many cases the materials have uses in biomedical applications, for example, in tissue engineering [8–10] or in developing self-assembled drug and gene delivery vehicles [11].

Lasic and Papahadjopoulos (pp 392–400) describe recent exciting developments in cleverly designed drug delivery systems currently used in biomedical applications consisting of self-assemblies of lipid and biocompatible polymer-lipids. Following this article, Bruinsma and Pincus (pp 401–406) describe our current theoretical understanding of protein–protein interactions leading to aggregation in membranes. Membrane-protein aggregation occurs in many vital biological processes including adhesion and cell–cell recognition events of the immune system. Their article is particularly timely as it builds on the considerable knowledge regarding the statistical mechanics of fluid membranes and the undulation interaction between membranes as originally described by Helfrich [12,13] and verified in numerous experiments during the last decade [14–23]. In contrast to the many studies of fluid membranes, there are very few experiments on solid membranes. Recent theoretical work on solid membranes, in particular, by Nelson and coworkers [24,25] and Aronovitz and Lubensky [26], has shown that in addition to the usual compression and shear elastic modes of a two-dimensional lattice, a third mode due to undulations and the effect of its coupling to the in-plane strains has profound implications. In the case of locally rough but globally flat tethered membranes, either thermally-induced or due to random quenched roughness, theory predicts the possibility of producing a novel new state of matter with anomalous elasticities [24–26]. These theories may turn out to describe the behavior of two-dimensionally ordered protein self-assemblies derived from bacterial coats [3,4] and two-dimensional red blood cell membrane skeletons [27].

Tirrell and Tirrell (pp 407–411) describe recent work on biopolymer syntheses which use extremely novel methods involving a combination of biological and chemical processes. As is evident from their article, a large gap exists between biologically produced materials and the polypeptides which can be produced synthetically, the best synthetic procedure being the ring-opening polymerization of α-amino acid N-carboxyanhydrides (NCAs). Chemical synthesis allows exceptional versatility in the types of amino acid monomers which can be utilized [28], yet the resulting polymers are almost exclusively homopolymers, random copolymers, or graft copolymers. To address these issues Deming [29] at the University of California at Santa Barbara is attempting to synthesize polypeptides via transition metal catalysis to control polymer end-group reactivity and prepare copolypeptides with controlled sequence and composition (e.g. diblock and triblock, and alternating copolymers) which will be able to self-assemble and display interesting properties.

Gittes and Schmidt (pp 412–424) bring the reader up to date on biological motors — a class of protein-based molecular machines — which are used in numerous cell-life processes involving the conversion of chemical energy into mechanical motion. The area of 'molecular-based bioenergetics' — the conversion of one form of energy

into another by utilizing molecular machines in general — has an unlimited potential in future biomolecular materials research [30]. Aside from the motors described by Gittes and Schmidt, researchers have been working with a large set of energy transducing machines. Bacteriorhodopsin, a membrane-protein from an Archeabacteria [2] converts light energy (photons) into electrochemical energy by pumping a proton across its membrane. The F_0F_1 ATPase complex (a membrane-associated protein localized in the thylakoid membranes of chloroplasts) converts the electrochemical energy of a proton into chemical bond energy in the synthesis of ATP [30]. These machines are extremely compact occupying volumes of order $(100\,\text{Å})^3$. Coupled molecular machines which convert one form of energy into another will most probably be utilized in future miniaturized robots. For example, a combination of such machines could be used to generate mechanical motion by an initial light (photon) trigger in a volume less than a cubic micron.

There have been, of course, numerous other very exciting developments in the past few years which will be outlined below. Tissue engineering is an extremely important and rapidly expanding field [8–10]. The goal of this research is to provide replacements for tissues and organs lost as a result of disease, aging, deformity, or accident. Among the current strategies are to seed a biodegradable polymer scaffold with desired cells and to optimize the conditions for cell proliferation. Once the tissue forms as a result of 'cell self-assembly', which usually involves molecular glues (i.e. cellular adhesion molecules), the plastic degrades. To date, artificial 'skin' and 'cartilage' have been successfully designed and used as replacement parts. This is an exciting research area that requires the participation of chemical engineers, complex fluid scientists, biologists and medical researchers.

In another area there have been new developments in the formation of new types of liposomes [31–36;P1] and emulsions [37–39]. Since their discovery, spherical liposomes (consisting of unilamellar or multilamellar vesicles) have received much attention because of their similarities to real cells and their encapsulation properties; they are likely to dramatically impact the medical field as drug and gene carriers as described in the article by Lasic and Papahadjopoulos. Recent groups have reported on the discovery of a new equilibrium phase of liposomes consisting of multilamellar tubular vesicles (L_{tv}) [31,32], not predicted by current theories describing fluid membranes. Among the very dilute phases which appear at equilibrium in surfactant solutions including the dilute lamellar L_α phases that are stabilized by the Helfrich undulation forces [14–21], the equilibrium L_4 phase of spherical vesicles [40,41], and the bicontinuous L_3 phases [42,43] all may be described by considering fluid membranes with physical properties described by Helfrich [12,13]. In contrast, the existence of the L_{tv} phase is not predicted with the Helfrich theory. Recent theoretical work which emphasizes a non-analytical bending energy term that appears to favor cylindrical and 'egg-carton' geometries may turn out to be the correct theory of the L_{tv} phase [44].

In a different vesicle system which is in a non-equilibrium regime, researchers have recently reported on a novel process for preparing multilamellar vesicles (MLVs) of controlled size [33–35;P1] These so called 'onion phases' are a result of a hydrodynamic instability when lyotropic lamellar phases are subjected to shear flow. The onion phases are currently used in cosmetics and chemical release applications [P1] and may have potentially important biotechnology applications. Under certain conditions, onion-like MLV phases may also occur spontaneously in mixtures of ionic and non-ionic surfactant membranes [36]. Dispersions made out of two immiscible liquid phases in the presence of surfactants are known as emulsions. By contrast with microemulsions, which form spontaneously, emulsions require external energy to form and are metastable. The intense interest in emulsion stabilization arises from their increased use in the cosmetics industries in formulations of lotions, gels, and creams. Recent novel new processing approaches to the development of emulsions made up of almost monodisperse droplets have paved the way for the unprecedented control of their stability and mechanical properties [37–39].

Recently, interesting results have been reported concerning biomolecular materials exhibiting higher-order self-assembly (i.e. self-assemblies of objects which themselves are self-assemblies of even smaller objects). Vesicles can be made to undergo a 'secondary' self-assembly into higher order structures in a controlled and reversible manner via 'site-specific' ligand–receptor coupling interactions [45,46]. The robustness, controlled versatility and reversibility offered by site-binding secondary self-assembly opens the way for the development of stable biomimetic structures consisting of microcompartments and membranes that could be designed to perform different functions (e.g. binding, biocompatibility, and controlled permeability and solute release) which cannot be easily carried out by single-membrane structures. Another example of the unexpected effects of higher-order self-assembly is the discovery of an exceedingly high temperature stable regime of the membrane-protein bacteriorhodopsin in stacked two-dimensional films [47–49]. The findings suggest general methods for the temperature stabilization of proteins and enzymes in artificially assembled multilayers of ordered arrays of biomolecules.

Some important new developments have occurred in the area of natural [50,51] and synthetic biogels [52]. Many biological cells experience shear stresses of order 100–1000 Pa. Their elastic resistance to such stress is largely due to a gel-like network of semiflexible actin filaments formed at the cell periphery. Despite some similarity of actin networks to conventional polymer gels

and rubbers, classical rubber elasticity cannot account for the large shear moduli required of the actin cortex *in vivo* and observed [50] for physiologic concentrations of actin solutions *in vitro* (1000 Pa for 10 mg ml^{-1}, whereas rubber elasticity would predict moduli of order 1 Pa). A novel new model for the elasticity of actin networks can account for both the magnitude of the shear modulus and its observed dependence on concentration and strain [51].

A recent discovery describes a new class of synthetic-based lamellar biogels made up of fluid membranes of lipids and surfactants with small amounts of polymer-lipids [52]. These gels are quite distinct from the 'onion-like' multilamellar vesicle phases which may also exhibit strong viscoelastic behavior with a finite yield stress [33–36;P1]. The gel phase is characterized by a highly defected microstructure made up of a network of connected membranes with the polymer-lipid stabilizing the high curvature regions, which on a semi-macroscopic length scale leads to random layer orientation domains. These lamellar biogels exhibit striking differences with isotropic hydrogels of polymer networks where the gel phase can be formed by adding water to the liquid-like lamellar phase, and, furthermore, gels with larger water concentrations require less polymer-lipid concentrations to remain stable. The underlying fluid membrane allows for the incorporation of membrane-proteins that are biologically active, thus providing a way in which to deliver such molecules in a stable gel.

In the next few years many researchers of biomolecular materials will almost certainly be working in the area of 'non-viral-based' gene therapy. Somatic gene therapy depends on the successful transfer and expression of extracellular DNA to the nucleus of eucaryotic cells, with the aim of replacing a defective gene or adding a missing gene in corrective molecular-level biomedical applications [53]. Although viral-based carriers of DNA are presently the most common method of gene delivery, there has been a tremendous recent surge in activity in the development of synthetically-based non-viral vectors. In particular, an important recent breakthrough involves the use of cationic liposomes (CL) as non-viral transfer vectors (i.e. carriers) of recombinant DNA molecules [54]. While significantly improved in transfection efficiency, compared to other non-viral carriers, at present, CL vectors exhibit much lower efficiencies than do viral vectors. This low efficiency is related to the lack of fundamental knowledge regarding the mechanisms which underlie transfection via cationic liposomes [53–56]. In particular, what is the precise nature of the interactions and resulting structures of the CL–DNA complexes? Also, what is the nature of the interactions of the complex with intracellular organelles and the mechanism of transfer across the nuclear membrane? Some recent experiments are now beginning to properly address the structure of the complexes through quantitative X-ray diffraction studies; they reveal a well defined higher-ordered liquid crystalline structure of the CL-DNA complexes (JO Radler, I Koltover, T Salditt, CR Safinya, unpublished data; DD Lasic, R Podgornik, H Strey, PM Frederik, personal communication). Meanwhile, on the theoretical side a recent elegant work shows that even in the absence of lipid self-assemblies, DNA molecules may have a tendency to condense into a new (as yet unobserved) state with a 'braided chiral' structure with crystalline order [57].

The obvious complexity in biomolecular materials research makes the field especially pleasing because of the seemingly unlimited number of very important unresolved problems. Furthermore, while almost no problem in this area will be completely solved due to its complexity, because of the importance of the field, even small progress towards their solution tends to lead to large gains from a scientific, technological, medical and environmental prospective. For future workers of this field it is important to realize that the highly interdisciplinary nature of the field means that physical and chemical scientists and engineers will only make real significant progress if they not only have an up to date appreciation of the relevant biological issues associated with the problem, but are also ready to invest a substantial amount of their research time working with biologists and medical researchers on some purely biological aspects of the problem.

Hard biological materials

The last few years have witnessed an increasing interest in the study of the strategies adopted by organisms in building their skeletal hard tissues, in order to provide scientists with ideas for the production of sophisticated artificial materials. Indeed, the world of biomineralization presents a varied range of solutions to the problems of scaffolding, support, abrasion and protection of soft tissues encountered by organisms of all species. These solutions, perfected over millions of years of evolution, are centered around the production of composite materials of minerals (amorphous or crystalline) and biological macromolecules. The uniqueness of these materials lies in the sophisticated control and construction strategies, rather than in the choice of the materials used.

The four remaining topics in this section cover the section on 'hard' biological materials, summarizing research performed on biomineralization and its synthetic counterparts, each from a different perspective.

Intuitively, the best way to fill a space with compression-resistant structural materials would appear to be to provide a solid space filling by *in situ* polymerization of readily available and transferable monomeric units. The amorphous precipitate may then be modelled into the desired shapes by accurate control of growth and aggregation of the polymer into nanometer- and micrometer-size particles. The strategy is adopted in biogenic silica materials and biomimetic silicate synthesis, reviewed here by Zaremba and Stucky (pp 425–429). The authors draw attention

to the extreme conditions required in the traditional synthesis of solgels and ordered silica-based materials, in contrast to the physiological conditions used by organisms. Moreover, although solgel-produced silica is industrially important, chemists have achieved little control over its physical properties. Therefore, new growth techniques, under organic preserving conditions, are sought after. Zaremba and Stucky review the biomineralisation techniques applied to silica synthesis and compare them to their biological counterparts. These include the introduction of organic frameworks such as surfactants, the use of *in situ* solid state phase transitions and *in situ* coassembly techniques.

Recent discoveries and characterization of biopolymers (proteins and carbohydrates) associated with biosilicates may result in a new model for biolsilicate formation. It is thus expected that biomineralization methods will be incorporated increasingly in silicate materials of the future.

The materials most widely used by organisms to build their hard parts, however, involve crystalline rather than amorphous minerals. Among these calcium carbonate and phosphate are the most studied. The use of such crystalline minerals has required the evolution of complex techniques to achieve complete control over their deposition. The interfacial aspects of these control techniques are reviewed by Hunter (pp 430–435). The processes of control over crystal orientation, nucleation, growth habit and polymorphism are examined separately in calcium carbonate and phosphate biomineralization and biomimetic crystallization. Interestingly, Hunter claims, in calcium carbonate biomineralization the control processes are reasonably well understood, although the organic matrix components are not well characterised. In contrast, the main proteins of bone, enamel and dentin (phosphate biominerals) have been sequenced, but a better understanding of the processes awaits consensus on the functions of the proteins involved. Hunter concludes that the rapid progress in elucidating events occurring at the organic matrix–crystal interface hold promise that a combination of techniques and approaches will soon produce a detailed understanding of mineralization in organisms "from mollusk to man".

From the egoistic human standpoint, understanding bone mineralization and the development of new bone biomaterials are a priority. Cuisinier (pp 436–439) examines the present degree of understanding of the initial events in bone crystal formation and the role of organic bone compartments in the control processes, with a view of the possible pathways for the development of bone biomaterials. A four stage development model is presented, mainly derived from HRTEM observations, which includes adsorption of ions, followed by formation of crystalline nanometer-size particles, their growth and lateral fusion. Work on matrix vesicles and some studies performed in cell cultures are also reviewed.

The question of how the final product of the biomineralization process fulfils its function is finally addressed by Currey (pp 440–445) in his review on micromechanics of biological hard tissues. Currey claims, and with good reason, that understanding the micromechanics of hard tissues has been hampered until recent years by the lack of a detailed understanding of their microstructures: a deficiency that is being rapidly remedied. From this starting point, Currey thus examines the current state of the art in the understanding of the microstructure in various vertebrate tissues. The mechanical parameters describing the material and its behaviour upon failure with microcrack formation are then considered. A review of the remarkable properties of other hard tissues, including nacre, enamel, and beetle wings follow. Currey concludes that biological materials have such complex microstructures that often they do not lend themselves to be studied with the tools developed for manmade composite materials. The transfer of information from biology to artificial materials should, however, yield valuable information about fabrication and micromechanics.

References

1. *Biomolecular materials.* Report of the University/Industry Workshop, US National Science Foundation report NSF 91-142 (1990).
2. Birge RR: **Photophysics and molecular electronic applications of the Rhodopsins.** *Annu Rev Phys Chem* 1990, 41:683–733.
3. Sleytr UB, Sara M: **Ultrafiltration membranes with uniform pores from crystalline bacterial cell envelope layers.** *Appl Microbiol Biotechnol* 1988, 25:83–90.
4. Baumeister W, Lemboke G: **Structural features of archaebacterial cell envelopes.** *J Bioenerg Biomembrane* 1992, 24:567–575.
5. Douglas K, Devand G, Clark NA: **Transfer of biologically derived nanometer-scale patterns to smooth substrates.** *Science* 1992, 257:642–644.
6. Schultz JS: **Biosensors.** *Sci Amer* 1991, 265:64–69.
7. Israelachvili J: *Intermolecular & Surface Forces*, edn 2. Academic Press; 1992.
8. Service RF, **Designer tissues take hold.** *Science* 1995, 270:230–231.
9. Langer R, Vacanti JP: **Tissue engineering.** *Science* 1995, 260:920–926.
10. Langer R, Vacanti JP: **Artifical organs.** *Sci Amer* 1995, 273:130–133.
11. Lasic DD: *Liposomes: From Physics to Applications.* Amsterdam: Elsevier; 1993.
12. Helfrich W: **Elastic properties of lipid bilayers.** *Z Naturforsch C* 1973, 28:693–703.
13. Helfrich W: **Steric interaction of fluid membranes in multilayer systems.** *Z Naturforsch A* 1978, 33:305–315.
14. Safinya CR, Roux D, Smith GS, Sinha SK, Dimon P, Clark NA, Bellocq AM: **Steric interactions in a model membrane system: a synchrotron X-ray study.** *Phys Rev Lett* 1986, 57:2718–2721.
15. Roux D, Safinya CR: **Synchrotron X-ray study of competing undulation and electrostatic interlayer interactions in**

fluid multimembrane lyotropic phases. *J Phys (Fr)* 1988, 49:307–318.

16. Safinya CR, Sirota EB, Roux D, Smith GS: **Universality in interacting membranes: the effect of cosurfactants on the interfacial rigidity.** *Phys Rev Lett* 1989, 62:1134–1137.

17. Porte G, Marignan J, Bassereau P, May RJ: **SANS diffuse pattern in very swollen lamellar phases.** *Europhysics Lett* 1988, 7:713–717.

18. Nallet F, Roux D, Prost J: **Dynamic light scattering study of dilute lamellar phases.** *Phys Rev Lett* 1989, 62:276–279.

19. Lei N, Safinya CR, Bruinsma RF: **Discrete harmonic model for stacked membranes: theory and experiment.** *J Phys II (Fr)* 1995, 5:1155–1163.

20. Ben-Shaul A, Gelbart W, Roux D (Eds): *Micelles, Membranes, Microemulsions, and Monolayers.* New York: Springer-Verlag, 1994.

21. Safinya CR: **Rigid and Fluctuating Surfaces: A Series of Synchrotron X-ray Scattering Studies of Interacting Stacked Membranes.** In *Phase Transitions in Soft Condensed Matter.* Edited by Riste T, Sherrington D. New York: Plenum; 1989:249–270.

22. Sackmann E: **Supported membranes – scientific and practical applications.** *Science* 1996, 271:43–48.

23. Lipowsky R: **The conformation of membranes.** *Nature* 1991, 349:475–481.

24. Nelson D, Piran T, Weinberg S (Eds): *Statistical Mechanics of Membranes and Surfaces.* Singapore: World Scientific; 1989.

25. Nelson DR, Peliti L: **Fluctuations in membranes with crystalline and hexatic order.** *J Phys (Fr)* 1987, 48:1085–1092.

26. Aronovitz JA, Lubensky TC: **Fluctuations of solid membranes.** *Phys Rev Lett* 1988, 60:2634–2637.

27. Schmidt CF, Svoboda K, Lei N, Petsche I, Berman L, Safinya CR, Grest GS: **Existence of a flat phase in red cell membrane skeletons.** *Science* 1993, 259:952–955.

28. Deming TJ, Fournier MJ, Mason TL, Tirrell DA: **Structural modification of a periodic polypeptide through biosynthetic replacement of proline with azetidine-2-carboxylic acid.** *Macromolecules* 1996, 29:1442–1444.

29. Deming TJ: **Controlled polymerization of α-amino acid-N-carboxyanhydrides using transition metal initiators.** *Polym Prep* 1996, 37:in press.

30. Rigaud J-L, Pitard B, Levy D: **Reconstitution of membrane proteins into liposomes – application to energy-transducing membrane proteins.** *Biochim Biophys Acta* 1994, 1231:223–246.

31. Chiruvolu S, Warriner HE, Narranjo E, Kraiser K, Idziak SHJ, Radler J, Plano RJ, Zasadzinski JA, Safinya CR: **A new phase of entangled giant tubular vesicles.** *Science* 1994, 266:1222–1225.

32. Klosgen B, Helfrich W: **Special features of phosphatidylcholine vesicles as seen in cryo-transmission electron microscopy.** *Euro Biophys J* 1993, 22:329–340.

33. Diat O, Roux D: **Preparation of monodisperse multilayer vesicles of controlled size and high encapsulation ratio.** *J Phys (Fr)* 1993, 3:9–14.

34. Diat O, Roux D, Nallet F: **Effect of shear on lyotropic lamellar phase.** *J Phys (Fr)* 1993, 3:1427–1452.

35. Panizza P, Roux D, Vuillaume V, Lu C-YD, Cates ME: **Viscoelasticity of the onion phase.** *Langmuir* 1996, 12:248–252.

36. Hoffmann H, Thunig C, Schmeidel P, Munkert U: **Surfactant systems with charged multilamellar vesicles and their rheological properties.** *Langmuir* 1994, 10:3972–3981.

37. Bibette J: **Depletion interactions and fractionated crystallization for polydisperse emulsion purification.** *J Coll Int Sci* 1991, 147:477–478.

38. Bibette J, Mason TG, Gang H and Weitz D: **Kinetically induced ordering in gelation of emulsions.** *Phys Rev Lett* 1992, 69:981–984.

39. Mason TG, Bibette J, Weitz D: **Elasticity of compressed emulsion.** *Phys Rev Lett* 1995, 75:2051–2054.

40. Kaler EW, Murthy AK, Rodriguez BE, Zasadzinski JAN: **Spontaneous vesicle formation in aqueous mixtures of single-tailed surfactants.** *Science* 1989, 245:1371–1374.

41. Safran SA, Pincus P, Andelman D: **Theory of spontaneous vesicle formation in surfactant mixtures.** *Science* 1990, 248:354–356.

42. Porte G, Marignan P, Bassereau P, May RJ: **Shape transformations of the aggregates in dilute surfactant solutions: a small-angle scattering study.** *J Phys (Fr)* 1988, 49:511–519.

43. Cates ME, Roux D, Andelman D, Milner ST, Safran SA: **Random surface model for the L3-phase of dilute surfactant solutions.** *Europhys Lett* 1988, 5:733–739.

44. Fournier JB: **Non-topological saddle-splay and membrane instabilities from rodlike cosurfactants.** *Phys Rev Lett* 1996, 76:4436–4439.

45. Chiruvolu S, Israelachvili J, Leckband D, Schmitt F-J, Walker S, Zasadzinski J: **Higher order self-assembly of vesicles via site-specific binding.** *Science* 1994, 264:1753–1756.

46. Ringsdorf H: **Molecular self assembly – snap together vesicles.** *Nature* 1994, 371:284.

47. Yi Shen, Safinya CR, Liang KS, Ruppert AF, Rothschild KJ: **Stabilization of the membrane-protein bacteriorhodopsin to 140°C in 2-dimensional films.** *Nature* 1993, 366:48–50.

48. Safinya CR, Rothschild KJ: **Self-assembly and protein stability.** *Nature* 1994, 370:105–106.

49. Hampp N: **Optical materials – heat-proof proteins.** *Nature* 1993, 366:12.

50. Janmey PA, Hvidt S, Kas J, Lerche D, Maggs A, Sackmann E, Schliwa M, Stossel TP: **The mechanical properties of actin gels. Elastic modulus and filament motions.** *J Biol Chem* 1994, 269:32503–32513.

51. MacKintosh FC, Kas J, Janmey PA: **Elasticity of semiflexible biopolymer networks.** *Phys Rev Lett* 1995, 75:4425–4428.

52. Warriner HE, Idziak SH, Slack NL, Davidson P, Safinya CR: **Lamellar biogels: fluid-membrane based hydrogel containing polymer-lipids.** *Science* 1996, 271:969–973.

53. Singhal A, Huang L: In *Gene therapeutics: methods and applications of direct gene transfer.* Edited by Wolff JA. Boston: Birkhauser; 1994.

54. Felgner PL, Gadek TR, Holm M, Roman R, Chan HW, Wenz M, Northrp JP, Ringold GM, Danielsen M: **Lipofection: a highly efficient, lipid-mediated DNA-transfection procedure.** *Proc Natl Acad Sci USA* 1987, 84:7413–7417.

55. Felgner PL, Rhodes G: **Gene therapeutics.** *Nature* 1991, 349:351–352.

56. **Gene therapy's growing pains. Special News Report.** *Science* 1995, 269:1050–1055.

57. Kamien RD, Nelson DR: **Defects in chiral columnar phases – tilt-grain boundaries and iterated Moire maps.** *Phys Rev E* 1996, 53:650–666.

Patent

P1. Diat O, Roux D, Laversanne R: **Process of making microcapsules.** International Patent WO9319735.

Stabilization of the membrane protein bacteriorhodopsin to 140 °C in two-dimensional films

Yi Shen*†, Cyrus R. Safinya*‡, Keng S. Liang†, A. F. Ruppert† & Kenneth J. Rothschild§

* Materials and Physics Departments, and the Materials Research Laboratory, University of California, Santa Barbara, California 93106, USA
† Exxon Research & Engineering Co., Annandale, New Jersey 08801, USA
§ Physics and Physiology Departments, Boston University, Boston, Massachusetts 02215, USA
‡ To whom correspondence should be addressed

Two-dimensional assemblies of membrane proteins (see ref. 1, for example) such as bacteriorhodopsin are of current interest because of their potential application in technological areas as diverse as molecular electronics and optical switching[2], molecular sieves[3,4] and the lithographic fabrication of nanometre-scale patterns[5,6]. Here we report that bacteriorhodopsin[7-9] can retain its folded native structure to temperatures as high as 140 °C when incorporated in multilayer structures of self-assembled, ordered films. Synchrotron X-ray scattering reveals that, under hydrated conditions, the two-dimensional lattice in multilayer films exhibits a reversible solid–liquid transition at about 69 °C, followed by irreversible denaturing of the bacteriorhodopsin at about 90 °C. But in dry films the melting transition and denaturation are suppressed up to 140 °C. These results suggest that it may be feasible to use multilayer assemblies of functional proteins and enzymes[10,11] in high-temperature applications.

The pioneering work of Blaurock, Oesterhelt and Stoeckenius[7-9] in the early 1970s led to the elucidation of the biological function of the integral membrane protein bacteriorhodopsin (bR). This protein functions as a light-driven proton pump and is involved in photosynthesis carried out by *Halobacterium halobium*, an extreme halophile (living in high salt environments) and a member of Archaebacteria[12,13] which thrive under conditions inhospitable to common eubacteria. Archaebacteria also include the high-temperature extreme thermophiles[12], which undergo optimal growth at around 90 °C and are stable to about 110 °C (ref. 12). To our knowledge, the structural stability of self-assembled bR at 140 °C, which we report here, is unprecedented for a folded protein, including those of the extreme thermophiles[12].

Unlike water-soluble globular proteins, membrane proteins[1] can be incorporated into a two-dimensional planar lipid membrane. In its native form, bR self-assembles into a two-dimensional crystalline purple membrane which is part of the plasma membrane of the bacterium. The initial X-ray scattering work[9] showed that the purple membrane, which has a diameter of ~0.5 μm and bilayer thickness of 49 Å, consists of trimers of bR which self-assemble in a hexagonal lattice with a spacing of 61.6 Å, with the remaining space filled by lipid (Fig. 1, top). Using electron microscopy, Henderson and Unwin[14,15] showed that each bR molecule (shown schematically in Fig. 1, top right) consists of a polypeptide chain that folds through the membrane to form seven α-helices; this is consistent with infrared dichroism measurements (see ref. 16, for example).

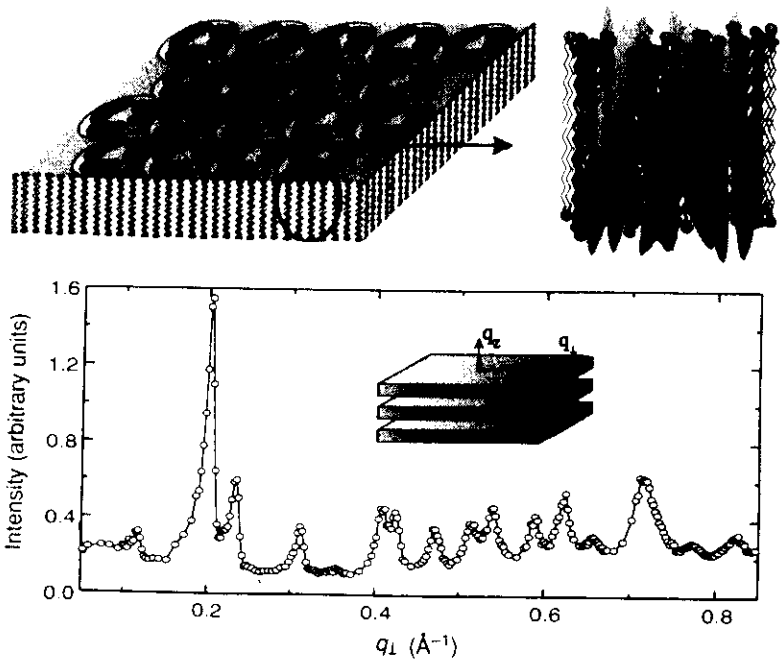

FIG. 1 Top, Schematic top view of the hexagonal lattice of the purple membrane composed of bacteriorhodopsin (bR) trimers with a blow-up of a side view (redrawn from refs 14, 15) of one bR molecule showing the seven α-helices that span the membrane. The purple colour resulting from the absorption of light by the purple membrane, which in its light-adapted form has an absorption maximum near 570 nm, is due to retinal covalently attached to bR (not drawn), found also in the visual pigment rhodopsin[7-9]. High-resolution cryoelectron diffraction[25] and spectroscopic techniques[26] have led to a more detailed 3-dimensional structure of bR and its retinal chromophore. Bottom, A typical X-ray intensity scan in reciprocal space along a direction parallel to the membrane plane through the many ordered peaks ((1, 0) through (4, 4)) of the 2-dimensional hexagonal lattice at 27 °C and relative humidity 60%. The inset shows the scattering geometry with respect to the multilayer orientation. Purple membrane was prepared from *Halobacterium halobium* R1M1 (ref. 27). A suspension of lyophilized purple membrane in distilled water (5 mg ml^{-1}) was centrifuged and 1 mg was spread on a thin 25-μm (hydrophilically prepared) silicon wafer transparent to X-rays and covering an area of diameter about 10 mm. The wet membrane/substrate preparation was then placed in a closed container and brought into equilibrium with deionized water at 100% relative humidity. This sample procedure yielded highly oriented ~10-μm-thick multilayer samples with a mosaic spread of the layer normals of ~15 deg measured through a standard crystallographic 'rocking curve' X-ray scan. The X-ray scattering experiments were carried out using both an 18 KW rotating anode X-ray generator, and at higher resolution, the synchrotron source at the National Synchrotron Light Source. Details of the experimental set-up have been described[28,29].

Figure 1 shows a typical X-ray intensity scan as a function of $q_\perp$ in reciprocal space parallel to the membrane at room temperature, through the numerous sharp in-plane peaks of the ordered hexagonal lattice of the purple membrane, with lattice spacing $a = 61.6$ Å. This highly developed two-dimensional ordering is in sharp contrast to the commonly occurring ordered L_β phases of membranes which comprise lipids for which normally only one or two low-order diffraction peaks are observed[17].

The temperature-dependent behaviour of multilayer stacks of purple membrane at high relative humidity is shown in Fig. 2. A (0, 0, q_z) scan (Fig. 2*A*) along the layer normal direction through the first six harmonics of the structure factor shows a very large interlayer spacing for the multilayer structure, with $d = 2\pi/q_1 = 196$ Å. Figure 2*B* includes plots of three in-plane scans: plot (a) shows the sharp (10), (11) and (20) peaks of the ordered phase below the melting transition at $T = 65.8$ °C, which are replaced by a broad peak of the liquid structure factor indicative of short-range positional order just above T_c in the disordered phase at $T \approx 69.2$ °C (plot b). Upon further heating to $T = 99$ °C (plot c), no remnant of the broad liquid peak is seen in the disordered phase. The melting transition of the two-dimensional bR lattice, which we found to be fully reversible, occurs at $T_c \approx 69.0$ °C. The slight shift in the position of the liquid peak towards lower $q_\perp$ values is consistent with a slightly less dense disordered phase with short-range positional order of the trimers of bR which make up the ordered phase. In contrast, the disappearance of the liquid peak for temperatures at around 99 °C, its irreversible behaviour when the liquid peak does not reappear upon cooling from this temperature, and the bleaching of the purple colour of the multilayer sample, are all consistent with the onset of denaturation of bR.

The behaviour under low-humidity conditions is entirely different and quite unexpected. The left panels of Fig. 3 show plots of the X-ray intensity under flowing nitrogen conditions, for scans along the in-plane direction (Fig. 3*a*), the q_z direction through the edge of the $q_\perp = (1, 1)$ scattering peak (Fig. 3*b*), and the multilayer stacking direction (Fig. 3*c*), both at room temperature and at $T = 132$ °C. The behaviour for temperatures within this range is essentially identical. The (0, 0, q_z) scans (Fig. 3*c*) show that the multilayer structure is unchanged from room temperature to very high temperatures at about 132 °C. The order–disorder transition, which occurs around $T = 69$ °C at high humidities (Fig. 2*B*), is suppressed entirely under these dry conditions as the membrane layers are forced to stack closely to one another.

Figure 3*d* compares high-resolution plots of the X-ray intensity under vacuum, for scans along the in-plane direction at $T = 76$ °C and 140 °C. The observation of sharp in-plane peaks of the $q_\perp$ scans of Fig. 3*a* and *d* is remarkable and shows that under dry conditions, the ordered hexagonal lattice remains intact up to temperatures as high as 140 °C. Furthermore, the fact that the X-ray structure factor intensities of Fig. 3*a*–*d* are essentially unchanged from room temperature to 140 °C indicates that bacteriorhodopsin remains in its tightly coiled α-helix conformation, with bR trimers self-assembled in the hexagonal lattice. We have observed a reduction in the degree of rehydration of multilayers previously exposed to these extreme temperatures of about 140 °C. This suggests that the membrane surface charge density associated with the hydrophilic amino-acid sections of bR protruding between layers is affected by these high temperatures. Although the self-assembled lattice is stable at these temperatures over several days, we found that at temperatures approaching 160 °C, bR denatures irreversibly over a period of a few hours, with the loss of the sharp diffraction peaks observed at 140 °C and of the purple colour.

Figure 3*e* shows, the visible absorption spectrum of three dry purple membrane samples measured at room temperature: curve 1 is for the sample at 23 °C (λ_{max} 560 nm), whereas the other two samples were cycled through 140 °C (curve 2, λ_{max} 567 nm), which resulted in a reduced intensity, broadening and slight red shift, and 160 °C (curve 3), where the sample bleached irreversibly and showed a flat visible band. The retention of the visible absorption at ~570 nm of all the dehydrated samples heated up to 140 °C contrasts sharply with hydrated purple membrane and

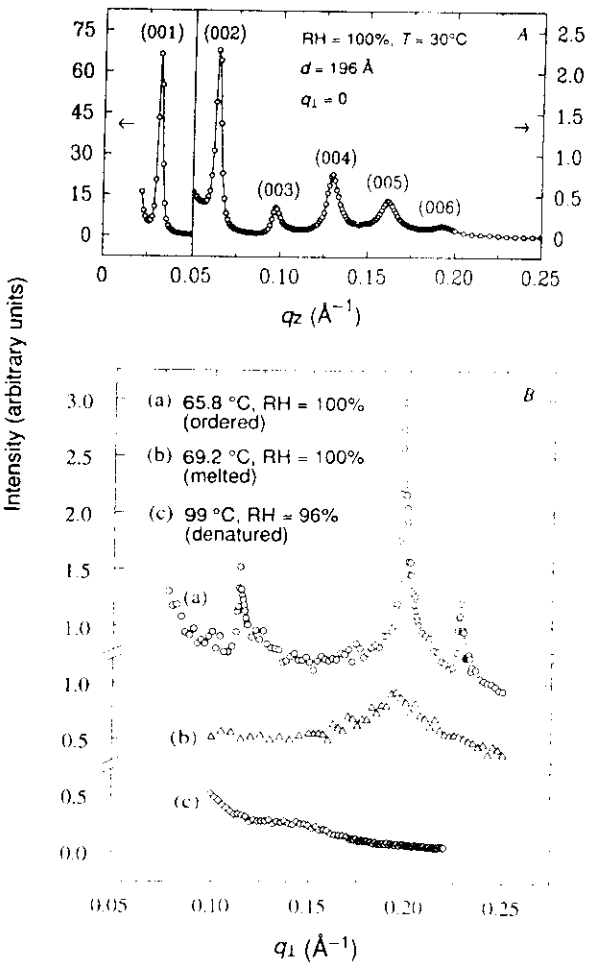

FIG. 2 High-resolution X-ray intensity scans on multilayers at high humidity (sealed in an X-ray capillary containing deionized water). *A*, *a* (0, 0, q_z) scan normal to the layers through the first six harmonics of the structure factor of the multilayer, which shows the large interlayer spacing with $d = 2\pi/q_1 = 196$ Å at 100% relative humidity (RH). *B*, In-plane scans parallel to the membrane plane: (a) the ordered sharp peaks below the melting temperature of the 2-dimensional hexagonal lattice ($T_c = 69$ °C); (b) the broad peak of the liquid structure factor of the disordered phase just above T_c; and (c) the absence of the liquid peak at higher temperatures when bacteriorhodopsin (bR) begins to denature and the membrane purple colour bleaches. Once denaturation (the coil–random transition of the α-helices) has set in, the behaviour is irreversible upon cooling. The broad peak around 0.13 Å^{-1} is from the tail of the (0, 0, 1) stacking peak which extends down to the $q_\perp$ plane because of the very large misorientation of the multilayer under these high humidity and temperature conditions. The scattering profiles are vertically shifted for clarity. Temperature control was about ±0.1 °C. These data are consistent with differential-scanning calorimetry studies of purple membrane dispersed in water basal salts or phosphate buffers[23], which indicated a transition of ~70 °C associated with the lattice melting[24], followed by a broad denaturation transition starting at ~90 °C.

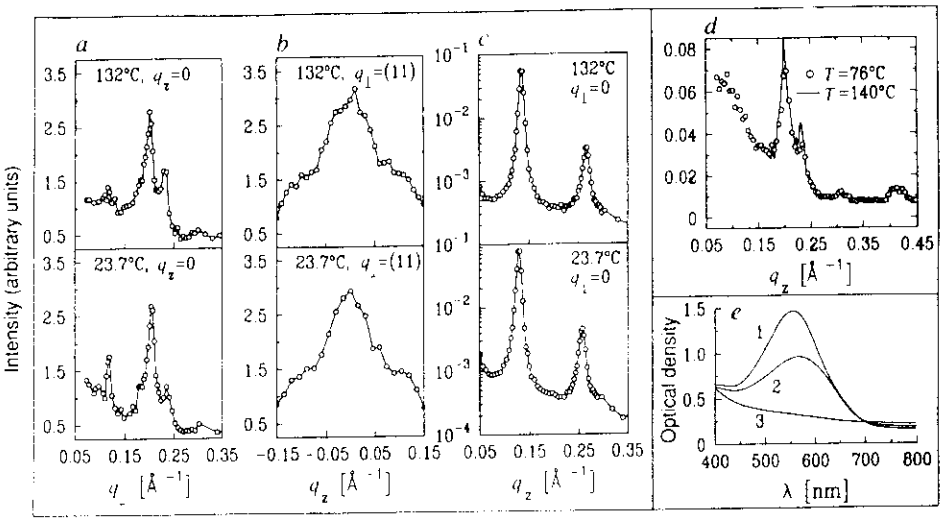

FIG. 3 Low-humidity (dry), low- and high-temperature data from multilayers of bacteriorhodopsin (temperature control was about ±0.1 C for nitrogen-dried samples, and ±0.5 C for samples under vacuum). *a*–*c*, X-ray intensity scans under flowing dry nitrogen at 23.7 and 132 °C: *a*, in-plane scans through the first four peaks ((10), (11), (20) and (21)) of the hexagonal lattice; *b*, q_z scans through the $q_\perp$ =(11) peak, showing a width much broader than those of the in-plane scan (*a*), which is indicative of the lack of interlayer positional correlations and arises entirely from the molecular form factor. This suggests that the suppression of the in-plane melting transition is not a result of the lock-in of interlayer positional correlations of neighbouring hexagonal lattices and a cross-over from 2-dimensional to 3-dimensional behaviour; *c*, (0, 0, q_z) scans along the layer normal are indicative of the well-defined multilayer nature of the samples, with interlayer spacing d = 48.5 Å at 23 C and 46.4 Å at 132 C. *d*, X-ray intensity scans along the in-plane direction under vacuum ($P \approx 10^{-8}$ torr) conditions at 76 and 140 C. Because of the sample holder configuration in our vacuum chamber, scans were recorded with the incident beam at grazing angles to the multilayer film. This resulted in the excess small-angle scattering originating from the substrate which swamped the (10) peak but allowed us to see the strong (11), (20), (21) and higher order peaks of the hexagonal lattice clearly. The sharp in-plane peaks (*a* and *d*) result from the highly ordered hexagonal lattice of bacteriorhodopsin which retains its structure to these very high temperatures (T = 140 C). *e*, Visible absorption spectrum of three dry purple membrane samples measured at room temperature. Curve 1: sample was held at 23 C; curve 2: sample cycled through and maintained at 140 C for 2 d; curve 3: sample cycled through and maintained at 160 C for 4 h, which resulted in bleaching. Samples were exposed to room light and then measured in a Varian 2390 spectrophotometer; measuring time was 45 min.

with bacteriorhodopsin reconstituted in various lipids and detergents, which exhibit an irreversible structural denaturation below 100 °C, that is characterized by a loss of visible absorption[18–20]. The proton-pumping activity of bacteriorhodopsin has not been measured in the high-temperature films, but the retention of the purple colour at 140 °C, together with the X-ray data, is strong evidence that the overall structure of the protein, the protonated Schiff-base bond attaching the retinal chromophore to the lysine residue at position 216, and the protein chromophore interactions[2,7–9], are all maintained. The partial red shift and broadening in the absorption of the high-temperature films is not unexpected and may be due to a shift in equilibrium of bR towards the 'O' intermediate, the last in the bR photocycle[2], which absorbs near 640 nm. A similar effect has been observed in purple membrane when the temperature is raised to 35 °C (ref. 21) and also in the mutant Tyr 185→Phe at room temperature[22].

Although it is not clear how the removal of water, which results in the forced stacking of the membrane sheets and the hindrance of out-of-plane fluctuations, suppresses the temperature-induced order disorder transition in purple membrane, it is likely that the absence of the melting transition enhances the stability of the protein structure at these unusually high temperatures around 140 °C. Our data suggest that the dehydrated two-dimensionally ordered phase of bR results in more extensive inter-protein interactions and a larger pressure of the ordered phase up to 140 C, relative to that of the corresponding liquid phase of bR found by us and others[23,24] above 70–80 C in hydrated multilayers. This then enhances the bacteriorhodopsin folding forces by exerting steric constraints that prevent protein structural changes, which otherwise would disrupt the bR α-helical bundle at these high temperatures. This is in agreement with previous results[18,20] which indicate that elimination of the crystalline lattice lowers the thermal stability of bR.

Aside from the direct potential applications to bacteriorhodopsin, we believe that our finding should lead to the stabilization of the structure of many other proteins and enzymes: that is, by artificially preparing multilayers of ordered arrays of macromolecules[10,11], significant high-temperature stability should be generated. Such stability will allow the investigation of the structure of a folded protein under these extreme temperature conditions. □

Received 12 July; accepted 21 September 1993.

1. *Electron Microscopy at Molecular Dimensions: State of the Art and Strategies for the Future* (eds Baumeister, W. & Vogell, W.) (Springer, Berlin and New York, 1980).
2. Birge, R. R. *Rev. phys. Chem.* **41,** 683–733 (1990).
3. Sleytr, U. B. & Sara, M. *Appl. Microbiol. Biotechn.* **25,** 83–90 (1986).
4. Baumeister, W. & Lembcke, G. *J. Bioenerg. Biomembr.* **24,** 567–575 (1992).
5. Douglas, K., Clark, N. A. & Rothschild, K. J. *Appl. Phys. Lett.* **56,** 692–694 (1990).
6. Douglas, K., Devaud, G. & Clark, N. A. *Science* **257,** 642–644 (1992).
7. Oesterhelt, D. & Stoeckenius, W. *Nature New Biol.* **233,** 149–152 (1971).
8. Oesterhelt, D. & Stoeckenius, W. *Proc natn. Acad. Sci. U.S.A.* **70,** 2853–2857 (1973).
9. Blaurock, A. E. & Stoeckenius, O. *Nature New Biol.* **233,** 152–155 (1971).
10. Uzgiris, E. E. & Kornberg, R. D. *Nature* **301,** 125–129 (1983).
11. Blankenburg, R., Meller, P., Ringsdorf, H. & Salesse, C. *Biochemistry* **28,** 8214–8221 (1989).
12. Brock, T. D. & Madigan, T. in *Biology of Microorganisms* 6th edn (Prentice Hall, New Jersey, 1991).
13. Woese, C. R. *Sci. Am.* **244,** 98–122 (1981).
14. Henderson, R. & Unwin, P. N. T. *Nature* **257,** 28–32 (1975).
15. Unwin, P. N. T. & Henderson, R. *J. molec. Biol.* **94,** 425–440 (1975).
16. Braiman, M. S. & Rothschild, K. J. *A. Rev. Biophys. biophys. Chem.* **17,** 541–570 (1988).
17. Smith, G. S., Sirota, E. B., Safinya, C. R., Plano, R. J. & Clark, N. A. *J. chem. Phys.* **92,** 4519–4529 (1990).
18. Brouillette, C. G., McMichens, R. B., Stern, L. J. & Khorana, H. G. *Proteins: Struct. Funct. Genet.* **5,** 38–46 (1989).
19. Kresheck, G. C. *et al. J. Photochem. Photobiol. B* **7,** 289–302 (1990).
20. Kahn, T. W., Sturtevant, J., Engelman, D. M. *Biochemistry* **31,** 8829–8839 (1992).
21. Fukuda, K. & Kouyama, T. *Biochemistry* **31,** 11740–11747 (1992).
22. Sonar, S., Krebs, M. P., Khorana, H. G. & Rothschild, K. *Biochemistry* **32,** 2263–2271 (1993).
23. Jackson, M. B. & Sturtevant, J. M. *Biochemistry* **17,** 4470–4474 (1978).
24. Hiraki, K., Hamanaka, T., Mitsui, T. & Kito, Y. *Biochim. biophys. Acta* **647,** 18–28 (1981).
25. Henderson, R. *et al. J. molec. Biol.* **213,** 899–929 (1990).
26. Rothschild, K. J., Braiman, M. S., Mogi, T., Stern, L. J. & Khorana, H. G. *FEBS Lett.* **250,** 448–452 (1989).
27. Oesterhelt, D. & Stoeckenius, W. *Meth. Enzym.* **31,** 667–678 (1974).
28. Safinya, C. R. *et. al. Phys. Rev. Lett.* **57,** 2718–2721 (1986).
29. Safinya, C. R., Sirota, E. B., Roux, D. & Smith, G. S. *Phys. Rev. Lett.* **62,** 1134–1137 (1989).

ACKNOWLEDGEMENTS. We thank S. Sonar and N. Patel for help with purple membrane preparation, R. Bruinsma, N. Clark, P. Pincus, T. Lubensky, D. Morse, D. Nelson, and S. Sonar for discussion and D. Thirumalai for critically reading the manuscript. The National Synchrotron Light Source (NSLS) is supported by the US Department of Energy. The Materials Research Laboratory at Santa Barbara is supported by the NSF. C.R.S. acknowledges the NSF for a biomolecular materials grant, and the Exxon Research and Engineering Company for a research grant. K.J.R. thanks the NSF and the ARO for support.

Heat-proof proteins

Norbert Hampp

PROTEINS are being exploited increasingly for technological ends, in biosensors and bioreactors for example. But some of these applications require high (more than 100 °C) operating temperatures, under which conditions many proteins are likely to denature. A striking exception is bacteriorhodopsin, as Shen *et al.* report on page 48 of this issue[1]. They found that in dry films bacteriorhodopsin was structurally stable up to a temperature of 140 °C. This is an astonishing result and an encouraging one for a new aspect of bacteriorhodopsin research — its use in optical information processing.

Approaching San Francisco by air, one obtains a spectacular view of the intensely purple basins of the salt works in the bay area. In the 1970s it was shown that the colour was largely due to a retinal-containing protein which could be isolated from bacteria living in the harsh conditions of a saturated solution of common salt, with little dissolved oxygen[2]. Survival in this ecological niche is possible because *Halobacterium salinarium* (formerly *Halobacterium halobium*) developed during evolution a set of proteins that enables it to use sunlight directly as an energy source. The key protein in the halobacterial photosynthesis is bacteriorhodopsin. Several tens of thousands of bacteriorhodopsin molecules form a two-dimensional crystalline lattice in the cell membrane over a region typically 500–1,000 nm in diameter and just 5 nm thick, the length of a single bacteriorhodopsin molecule. From its colour, this membrane fragment is called a 'purple membrane' and may be considered as the biological solar cell of the halobacterium. Each single bacteriorhodopsin molecule in the purple membrane acts as a light-driven proton pump. After absorption of a photon, bacteriorhodopsin transports a proton from the inside of the cell to the outer medium and thereby converts light energy into chemical energy which enables the halobacterial cell to survive.

When we talk of bacteriorhodopsin's inertness towards chemical and photochemical degradation and its remarkable longevity, we should qualify this: it is the purple membrane form that we mean. Purple membranes contain about 10 lipid molecules per bacteriorhodopsin acting like a glue for the bacteriorhodopsin trimers. Solubilization of the membrane and analysis of the isolated trimeric or monomeric bacteriorhodopsin indicates that the intact membrane is crucial for the stability of the material. Shen *et al.*[1] have identified another key aspect, the absence of water, in maintaining stability above 100 °C, extending the utility of purple membranes at the high temperatures demanded for technical applications.

Bacteriorhodopsin combines three functions that in principle are technically useful (see figure)[3]. First, it is a light-driven proton pump, so might be exploited to convert sunlight into chemical or electrical energy. Second, it has photoelectric properties due to the initial charge separation in the molecule after absorption of a photon. Third, it is a photochromic protein: absorption of light leads to a reversible colour change from purple to yellow. It can be switched back and forth with blue and yellow light more often than any other known chemically synthesized photochromic compound. This and the fact that bacteriorhodopsin uses light very efficiently (just 1–2 photons are needed to switch a single molecule from purple to yellow) make it attractive for optical information processing.

Two decades of interdisciplinary research have pinned down the structure[4] and molecular function[5,6] of bacteriorhodopsin fairly precisely. Deliberately mutated bacteriorhodopsin molecules were first obtained in *Escherichia coli*[7]. With the development of a halobacterial transformation system[8] it has become possible to obtain the mutated bacteriorhodopsin molecules in the stable purple membrane form and in bulk. Dry films of some functionally modified bacteriorhodopsins have already proved useful in optical information processing, for example in holographic pattern recognition[9]. The optical properties of dry bacteriorhodopsin films might produce different technical applications[10]. Thermal denaturing has never been a problem, but nobody has tried to push dry bacteriorhodopsin films to the limits. The results of Shen and co-workers place them well into a temperature range that is adverse for most synthetic photochromic materials, especially in the presence of oxygen and light.

With luck, their work will encourage others to transform 'well characterized' biological macromolecules into the solid or glassy state (not, in general, as easy as with purple membrane) and to investigate the conformational stability of the resulting material at higher temperatures. □

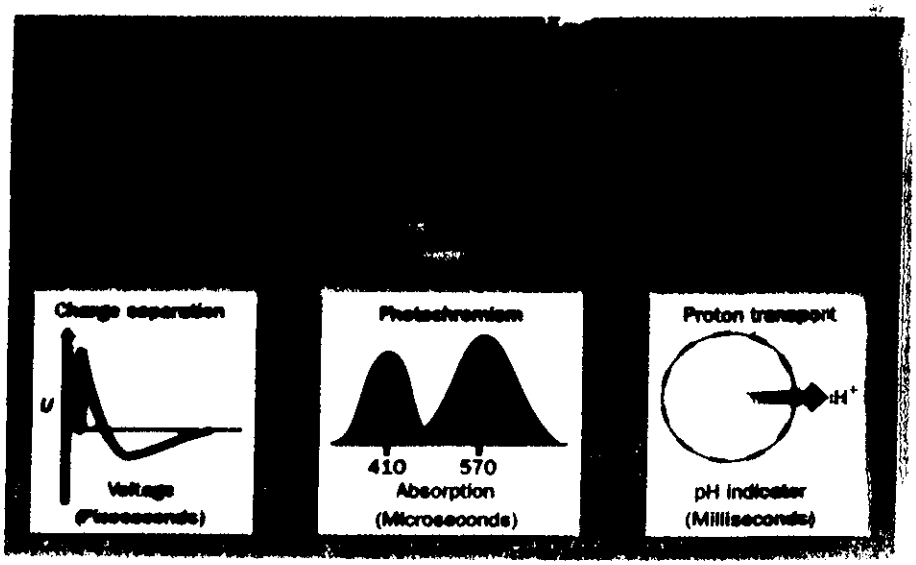

Bacteriorhodopsin consists of a single strand of 248 amino acids arranged as seven α-helices (blue) and a covalently attached retinylidene residue (purple). Absorption of a photon leads to the transport of a proton through the protein pore of bacteriorhodopsin. This process divides into (1) an initial isomerization and charge separation on the picosecond timescale, (2) a reversible colour change on the microsecond timescale and finally (3) the proton transport which can be observed by means of pH indicators. A complete proton transport cycle of bacteriorhodopsin takes about 10 milliseconds. Each of these basic phenomena is of potential technical use.

Norbert Hampp is at the Institute for Physical Chemistry, University of Munich, Sophienstrasse 11, D-80333 München, Germany.

1. Shen, Y. *et al. Nature* **366**, 48–50 (1993).
2. Oesterhelt, D. & Stoeckenius, W. *Nature new Biol.* **233**, 149–152 (1971).
3. Oesterhelt, D. *et al. Q. Rev. Biophys.* **24**, 425–478 (1991).
4. Henderson, R. *et al. J. molec. Biol.* **213**, 899–929 (1990).
5. Stoeckenius, W. & Bogomolni, R. A. *Rev. phys. Chem.* **34**, 693–733 (1983).
6. Zimanyi, L. *et al. Biochemistry* **31**, 8535–8543 (1992).
7. Braiman, M. S. *et al. J. biol. Chem.* **263**, 9271–9276 (1987).
8. Ni, B. F. *et al. Gene* **90**, 169–172 (1990).
9. Thema, R. & Hampp, N. *Opt. Lett.* **17**, 1158–1160 (1992).
10. Hampp, N. *et al. Mat. Res. Soc. Bull.* **17**, 56–60 (1992).

Proteins (macromolecules) within Membranes

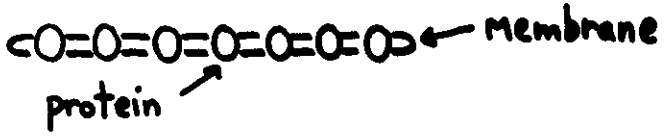

Structures / Interactions / Protein shape stability

Macromolecules associated with Membrane Surface

polymers with oily anchor :

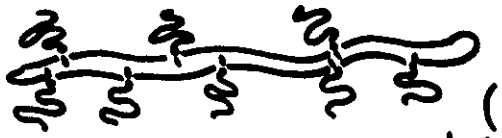

- models of carbohydrate coats of cells
(biology of sugar groups related to specific adhesive

- what are the relevant (non-specific) interactions ?.
- applications: drug / gene carriers

DNA / DNA-Complexes ⟷ bound to Membranes

- statistical mechanics: polymer on fluctuating membr

- biology / gene therapy & therapeutics:
How do nucleic acids interact with / cross membr

Self-Assembled Protein Lattice :

Synchrotron studies:
phase behavior; ordered-disordered; protein stability

statistical mechanics: Ordered membranes ; d=3

 height fluctuations :

-anomalous elastic constants (e.g. μ (shear) → 0; liquid blue

Probe $S(\vec{q})$, μ (interactions) in Complex System

Biomolecular materials: activity derived from protein

Heat Proof Proteins

Bio-gels

Biology: 2-dimensional protein crystallography
(low-dimensional T-fluctuations ignored)
— function : membrane protein T-stability
denaturation
(relation to structural nature of self-assembly
(interprotein interactions))

Red Blood Cell (~ simple cell)

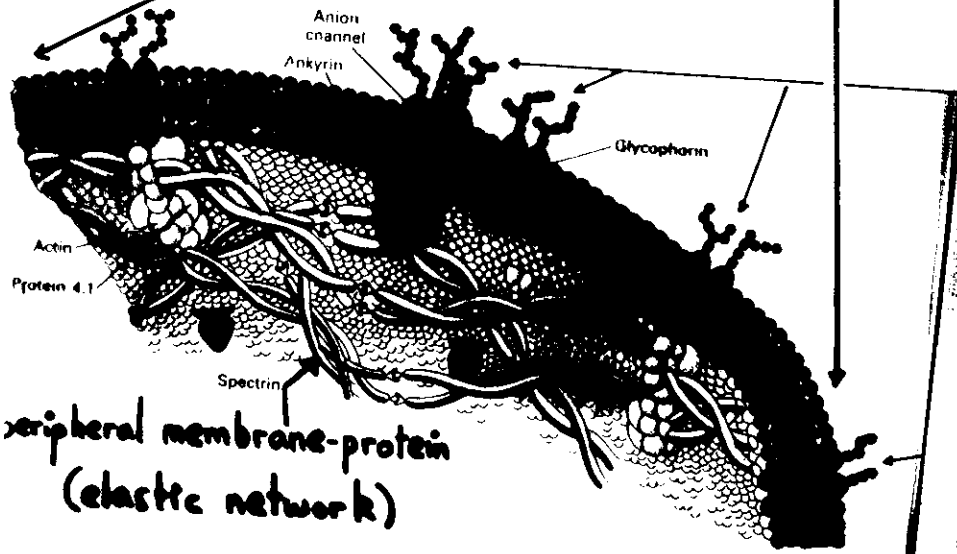

peripheral membrane-protein (elastic network)

(Membrane Associated Proteins)

■ Integral membrane proteins

Membrane Protein Bacteriorhodopsin

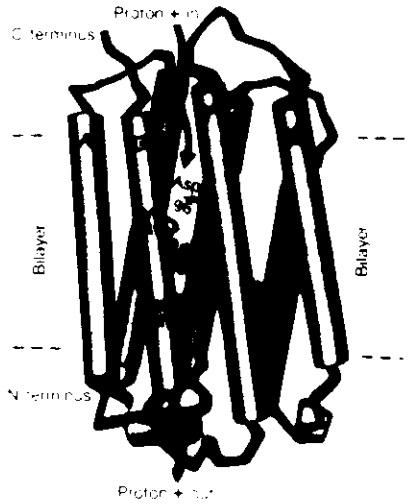

From D.L.D. Casper (Brandeis University)

Photon-induced Proton Pump

3 Functions of the Membrane Protein Bacteriorhodopsin

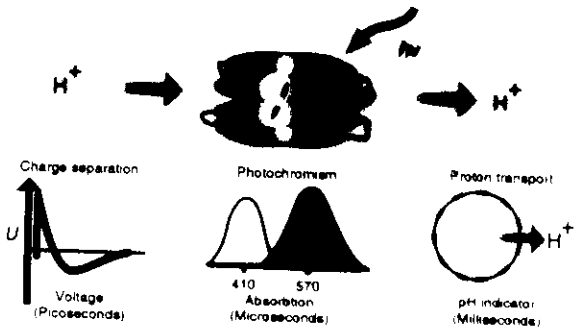

From Norbert Hampp (Institute for Physical Chemistry, University of Munich)

Halobacteria (Salt loving)

W. Stoecken
D. Oesterh
A. Blaur

d Shaped,
lt lakes →

Surface (S) Layers (outer Coat, "crystalline")

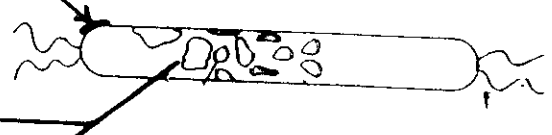

"Crystalline" patches (Purple Membrane; photos
(inside plasma membrane)

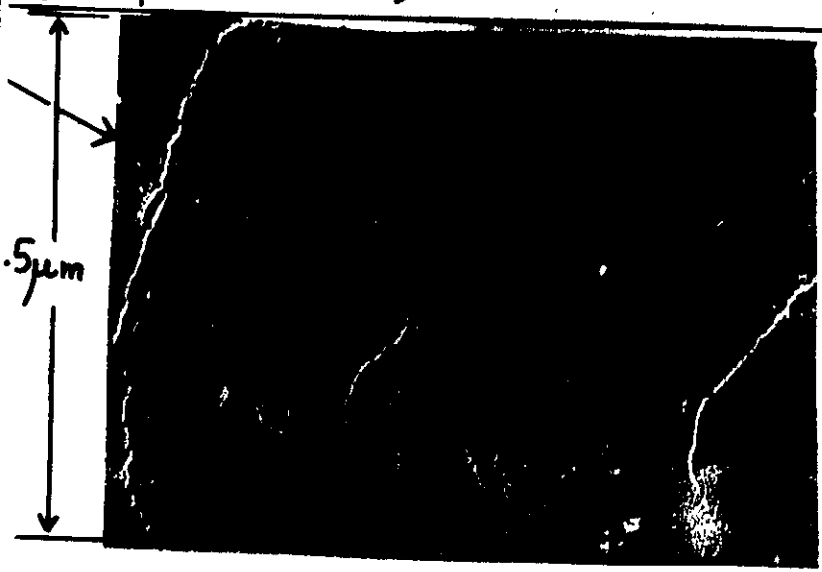

e-micro
cracks:
hexago
lattice
planes
(inter
at 60°,

Purple Membrane:

Bacteriorhodopsin (bR)

lipid

side view:

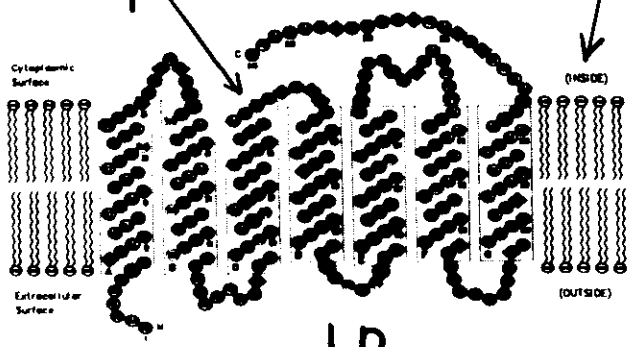

bR

top view:

protein-lattice

(trimers of bR)

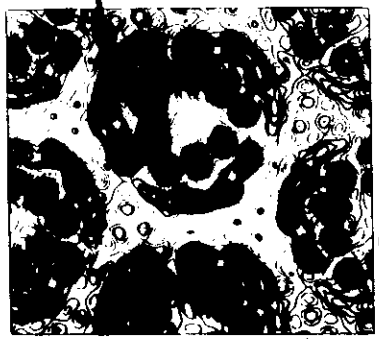

(density map)

hexagonal

bR: light induced proton pump (photoelectric)
(molecular solar cell)
(bioelectronics)

eversible Protein Self Assembly (non-covalent bonds)

-layers: 3 bacterial species

(outer crystalline coat ~ common feature)

gomer

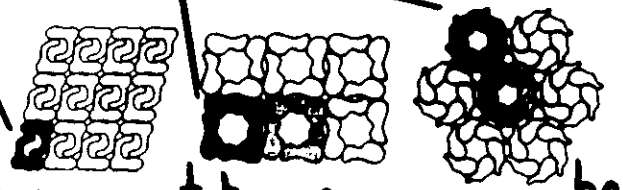

dimer tetramer hexamer

M. Sára
U. Sleytr

tice: Oblique square hexagonal

(lattice spacing: 5 → 30 nm)

- Pore size: nanometer range, species dependent
- Applications:
  - Molecular sieve (membrane separations)
  - Nanometer scale patterns (lithography)

Experiments: Multilayer Stacks: Charged sheets in H_2O

phase behavior: ordered | disordered [denaturation]

protein function: "ON" | "OFF"

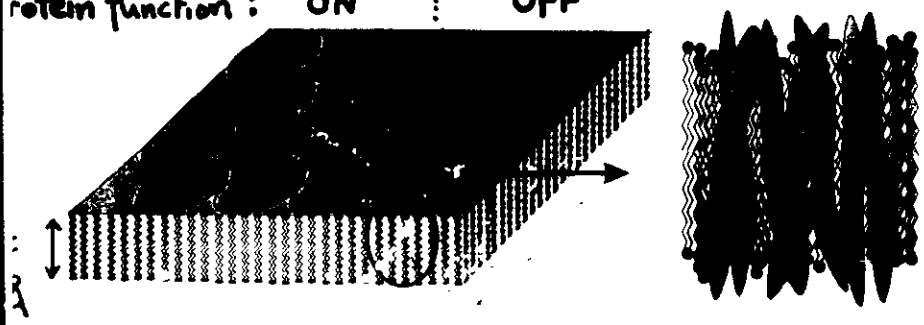

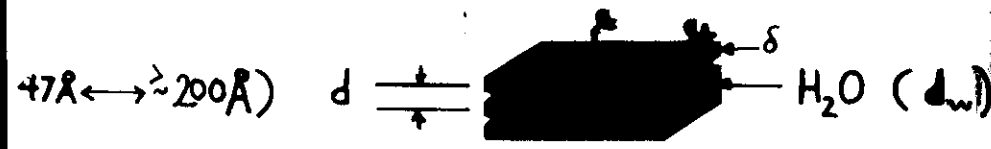

Control parameters:

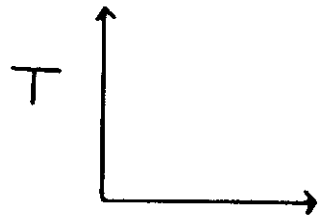

Relative humidity ($d = d_w + \delta$)

(sets d_w = amount of H_2O)

Structure inside membrane sheet:

2-dimensional (hexagonal)

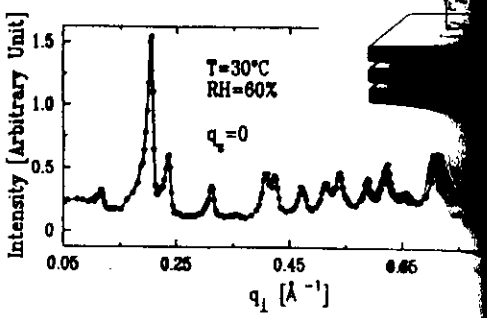

High Resolution : Synchrotron

protein lattice

- Asymmetric line-shape: (A)

  2D scattering of partially oriented sheets

- Broad q_z "rod scan": (B)

  no interlayer positional correlations

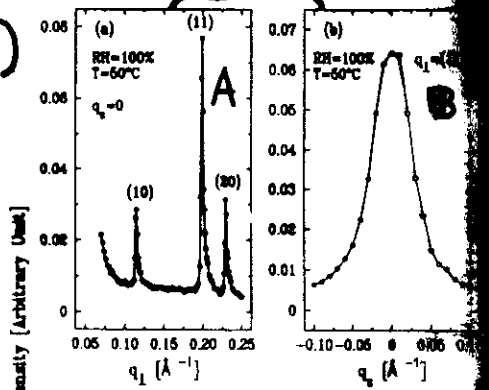

membrane stacking

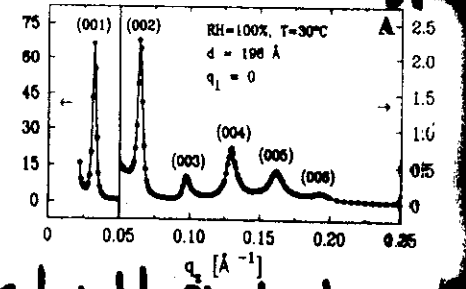

- 2D solid membrane embedded in 3-dimensions

(confined between neighbors, height fluctuations

Melting of (bacteriorhodopsin) protein lattice:

at relative humidity = 100%

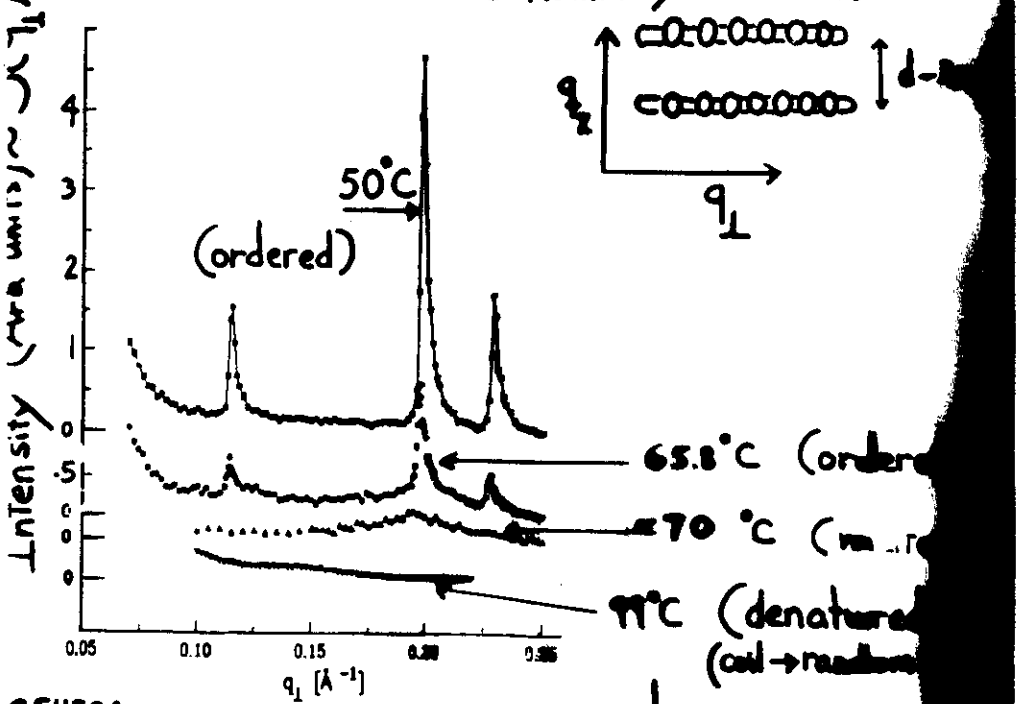

asure:

$S(q_\perp) \sim 1/|\vec{q}_\perp - \vec{G}|^{2-\chi_G}$ ← (real space: $\langle \rho_G(R)\rho_{G'}(0)\rangle \sim \frac{1}{R}$

$\chi_G = \frac{k_B T G^2}{4\pi\mu} f$ ($1 < f = \frac{3+\lambda/\mu}{2+\lambda/\mu} < 2$)

μ (shear modulus) $\propto 1/\chi_G$ (Lamé constants $\lambda+\mu =$

many diffraction peaks (to large $\vec{G}$) ⟩ χ_{G_n} small ⟩ μ Large, Rigid Lattice

Melting of 2D lattice : (Kosterlitz-Thouless)

defect = dislocation

(Burger's vector $\vec{b}$)

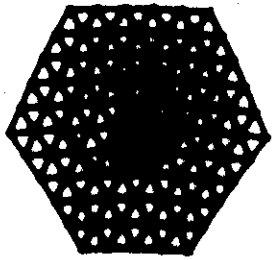

$K_0 = 4\mu \frac{1+\lambda_{2D}}{2+\lambda_{2D}}$

Young's mod

dislocation energy : $K_0 b^2 \ln(R/a) = U_d$

dislocation entropy : $k_B \ln (R/a)^2 = S_d$

Melting (T-induced "unbound" dislocations)

$U_d \sim T S_d$

KT model : $K_0^{melt} = 16\pi \frac{k_B T}{a^2}$, 2D melting con

$\mu = 6\pi k_B T$ $(\mu = \lambda)$

bacteriorhodopsin lattice in multilayers :

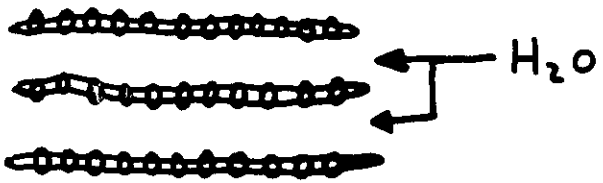

2D membrane confined between walls

---

i.e. behavior between

2D (flatland) & 2D "free" in a

What is behavior "free" membrane?

2D membrane in a solvent (size R)

)

ifined in
= 2

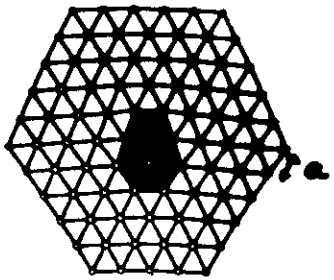

$U_d = K_0 b^2 \ln(R/a)$

K_0 = Young's mod.

) Free to Buckle (height fluctuation) (Seung-

change:

-plane elastic energy

r bending energy

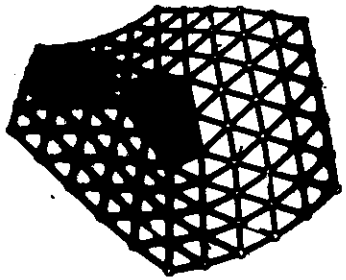

$U_d = E_c\left(1 - \text{const}\frac{R_b}{R}\right)$ finite! R_b = buckling radius $\sim \frac{K}{\gamma}$

$TS_d > U_d \Rightarrow$ **Buckled membrane is melted hexatic phase, $T \neq 0$**

bacteriorhodopsin (bR) has 2D ordered phase & finite T_c :

however:

δ

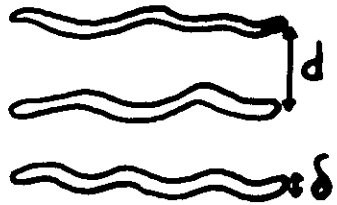

confined between neighbors

Confinement stabilizes ordered phase (Morse-Lubensky)

ect
t:

buckled membrane ↓ finite

flat membrane ↓ log. divergence)

Truly confined 2D limit : remove solvent

Increasing temperature,
Relative Humidity ≃ 0
(DRY AXIS)

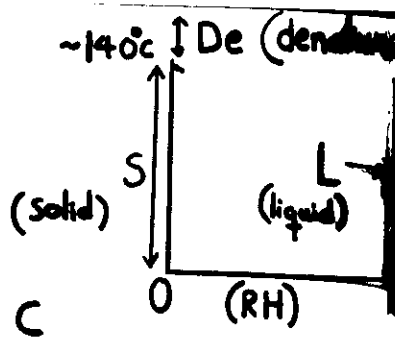

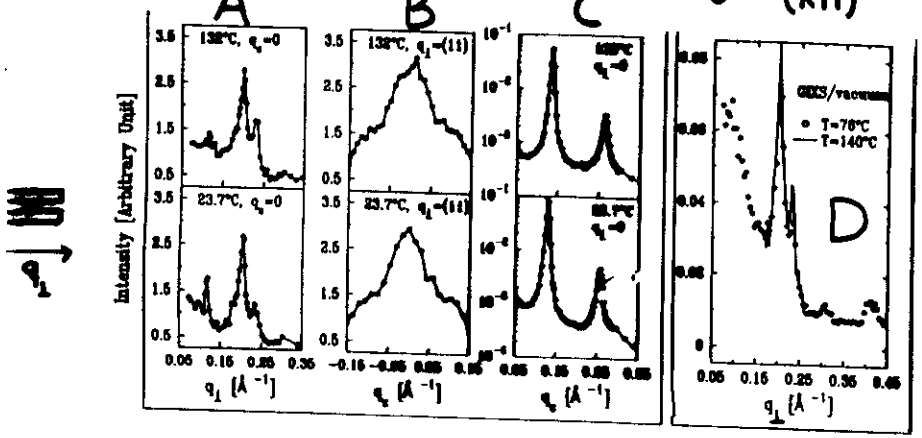

Protein-lattice (2D Solid↔Liquid) transition sup
. buckling (height fluctuations) hindered (A, D)

2D lattice not correlated between layers (B)

T_c (Dry) > 140°C

Consistent with large μ, & confinement induced or

Recall data show $\frac{\mu}{k_B T} \gg 1$, $T_c - T \simeq 10°k$

i.e. Flat 2D solid should not melt

- Buckling induced height fluctuations – out

- Solid ⟶ Liquid melting transition (at cond
d_w = hydration) suggests height fluctuations
(protein protrusions) at ≈ 5 Å (e.g. break
of trimer bonds) leading to impurities (monomers)
and melting. (Suppression of $\langle h^2 \rangle$ at ≃ 5 Å lev
moves melting transition.)

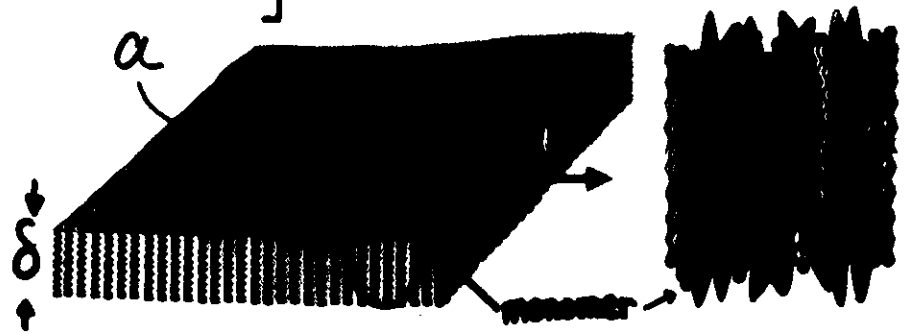

What about $T_c(q)$ which shows smooth be
For $d_w \gtrsim 5$-10

nter layer Interaction induced intra-membrane melting
(Parsegian; Goldstein-Leibler)

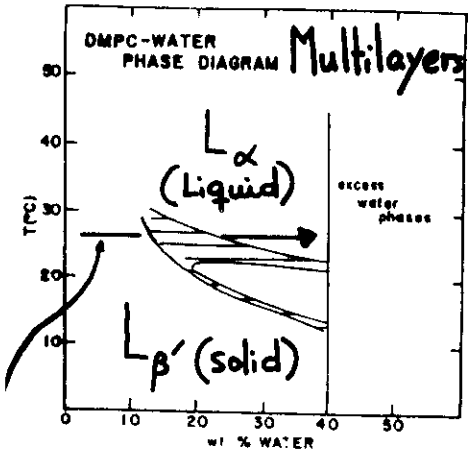

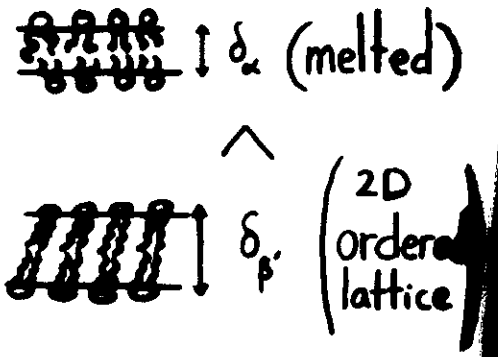

pts:

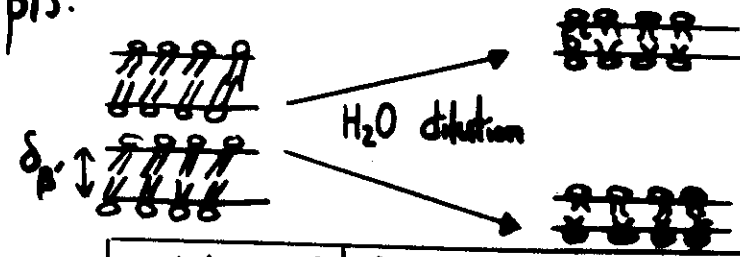

Dilution (d_w ↑) squeezes membrane (δ ↓)
→ chain melting

ptical data:

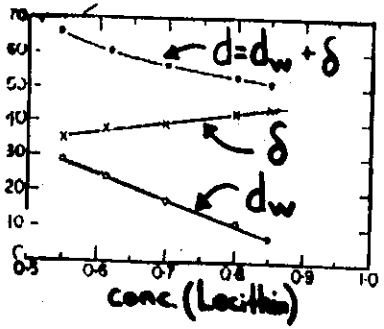

- Parsegian: Repulsive inter
interaction gives this
(independent of origin o
repulsion; hydration, el

Experimental Control: d_w

Stacking at different hydration levels (~ stacks under pressure

- **Experimental Findings**

) measurement of Protein-lattice rigidity { μ-dete
from pr
protein

) d_w controls T_c ⇒ control of inter-protein

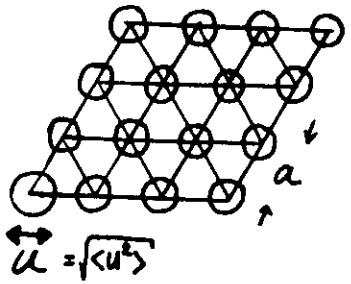

Lindemann melting condition

$u \sim 0.1\, a$ $(T = T_c)$

$u = u(\mu(d_w), \lambda(d_w); K(d_w))$
↑ shear ↑ bend

Structural nature (i.e. solid, liquid) of self-assembly:

↓

Control of m-protein stability
(denaturation access only from Liquid phase)

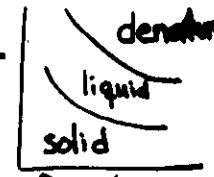

– inter protein forces contribute to protein folding { Protein-
biomate

Heat-proof proteins

[Shen et al., Nature
v364, 48 (1993)
[Safinya & Rothst
v370, 105 (199

Higher order self-assembly

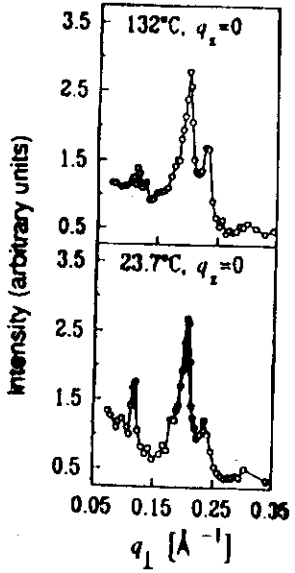

X-ray diffraction

leads to
high temperature stability

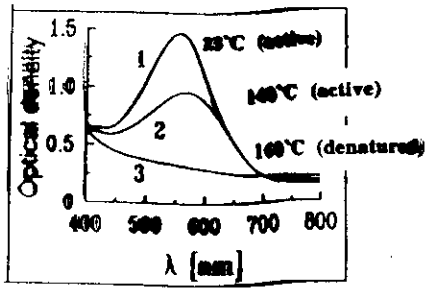

Optical measurement

Future directions :

- high temperature enzymes
- temperature stable molecular sieves

-Protein Folding Forces at high T.

Heat-proof proteins

Protein stabilization by higher order self-assembly:

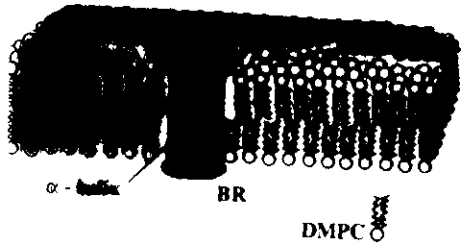

"gas phase" $T_{denature} \approx 40°C$

2D-monolayer $T_{denature} \approx 90$

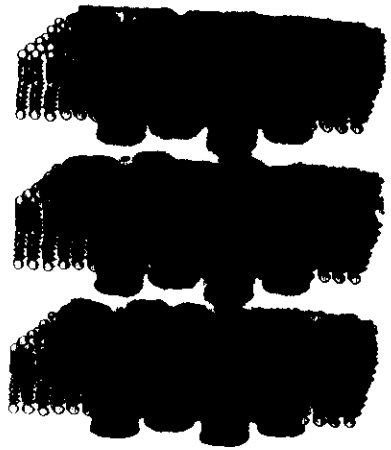

stacked 2D-monolayers $T_{denature} > 140°C$

Temperature Stabilization of Functional Proteins:

- Biosensors (Toxin Detection)
- Bioreactor Molecular Selves (Purification of Genetically Engineered Proteins)
- Catalytic applications (PCR Machine)

(i) Protein/Complex fluid complexation

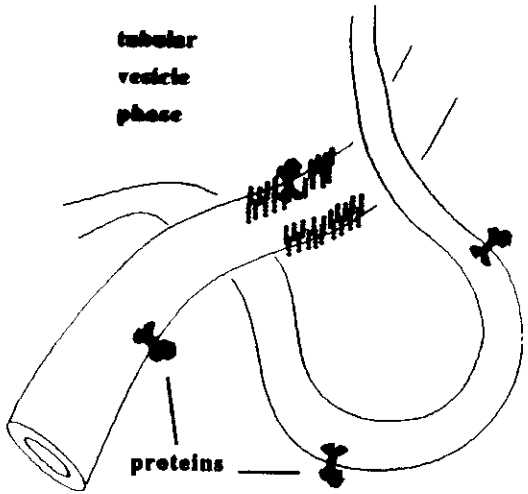

bicontinuous, sponge-like phase

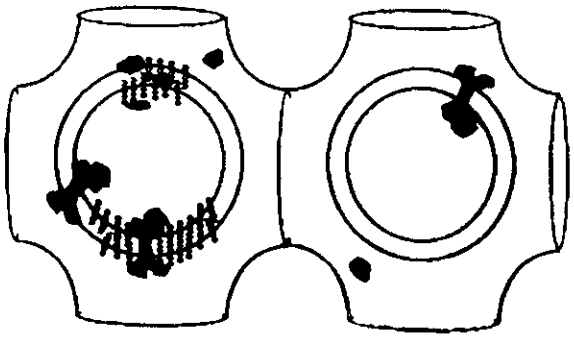

Giant Tubular Vesicles

Heidi Warriner, G. Subramanian, Stefan Idziak, Joachim Radler, Cyrus Safinya (Materials)
S. Chiruvolu, Ed Naranjo, Joe Zasadzinski (Chemical Engineering)

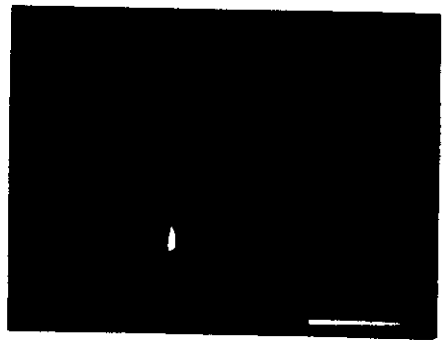

DIC 10 μm

x 1000

DMPC
geraniol
water

10 mm

x 50

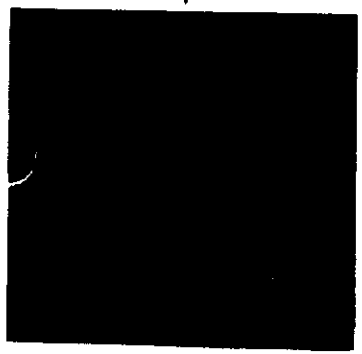

Cryo TEM 100 nm

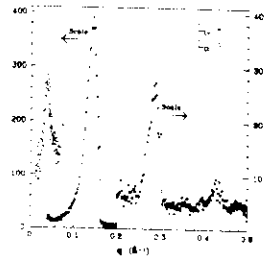

X-ray

Liquid Crystal
of tubular vesicles

- Cosmetics: liposomal formulations in creams, gels.
- drug, gene delivery
- Present work: Liquid crystal phases of giant tubular vesicles

Science **266**, 1222-1225 (1994)

Lamellar Biogels: Fluid-Membrane-Based Hydrogels Containing Polymer Lipids Making Gels by Adding Water

Heidi Warriner, Stefan Idziak, Nelle Slack, Patrick Davidson, Petra Eiselt, Cyrus Safinya (UCSB)
Hans-Werner Schmidt (Bayreuth, Germany)

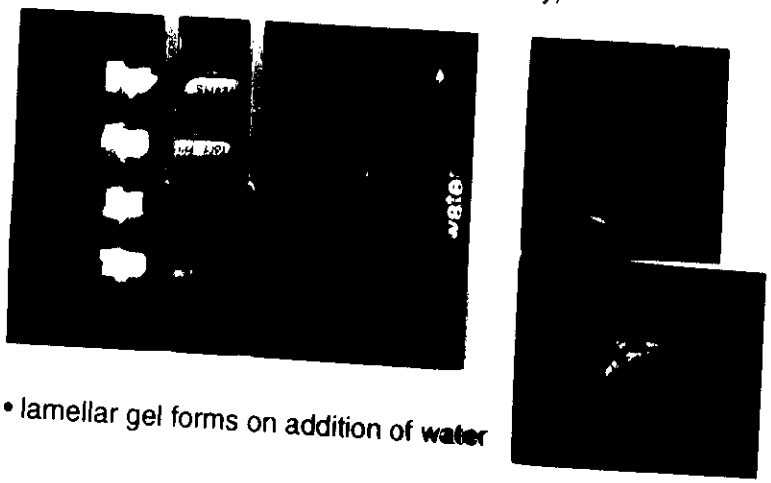

- lamellar gel forms on addition of **water**

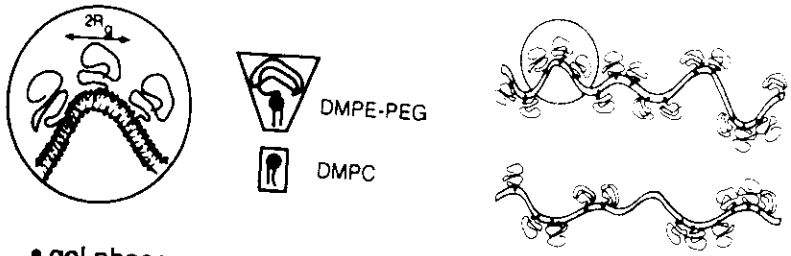

- gel phase contains no solid component
- Bioactive gels
  tissue healing, drug delivery

Science, **271**, 969-973 (1996).

Polymer Modification of Biomolecules

- **Peptide/Protein-hydrophilic Polymers:** (e.g. Amgen)

  extension of blood circulation times of therapeutic proteins/peptides (e.g. bGH, insulin).

  Hydrophilic polymer "protects" proteins against immune system. (Peptide and Protein Drug Delivery, ed. V.H.L. Lee)

- **PEG-lipid** (Initial work: T. Allen, D. Papahadjopoulos, D. Lasic)

  Liposomes as macromolecular (drug, gene) carriers

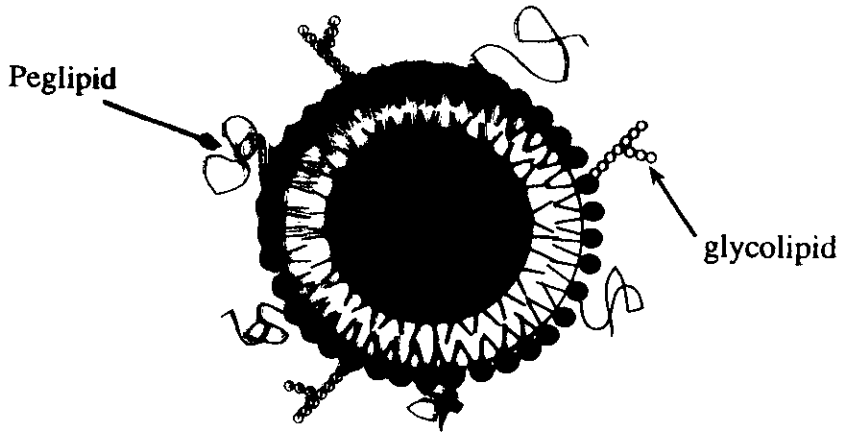

Stealth (sugar, polymer-coated) Liposomes (e.g. L.T.I.)
Partial avoidance of immune system

Steric stabilization through polymer-brush repulsion (Lasic et al.; Needham, McIntosh)

Force Measurements (T. Kuhl, J. Israelachvili)

} fully (polym... coated lip...

Experiments: Polymer Coated Membranes

Components:

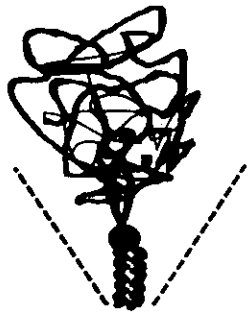

DMPE-PEG

DMPC

Pentanol

Water

lamellar L_α:

Fluid Bilayers)

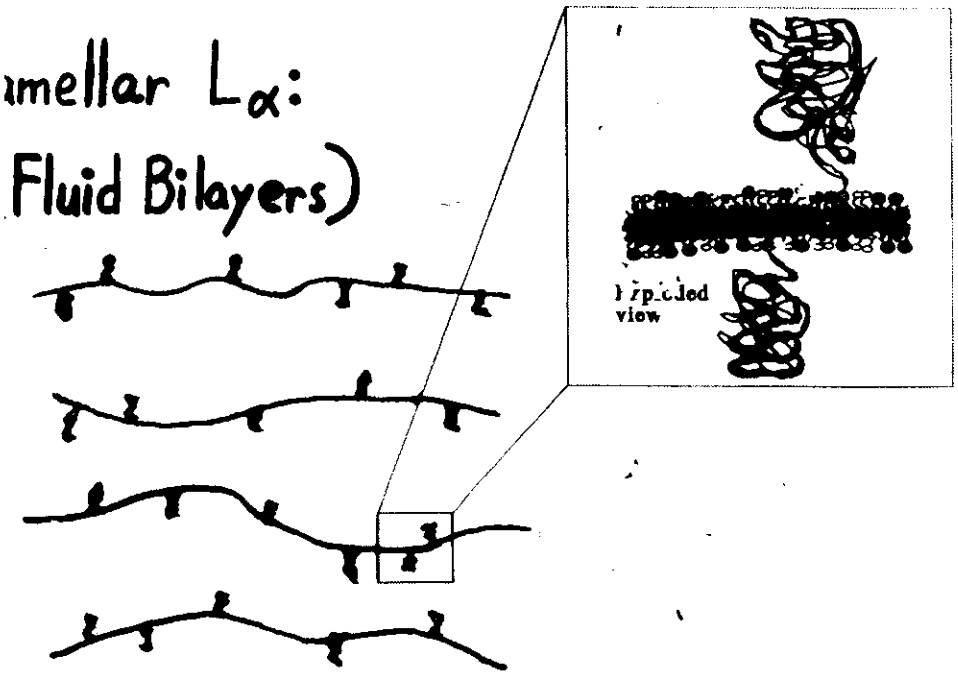

Polymer Coated Membranes:

key ingredients:

(a) FLUID membrane (allows **lateral** mobility of peg-lipids.)

(b) bare membrane (without the polymer coating) is stabilized through repulsive undulation forces.

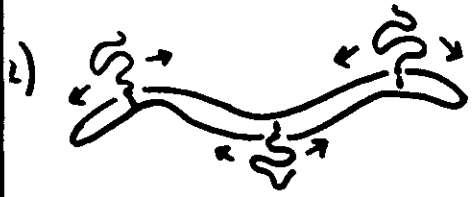

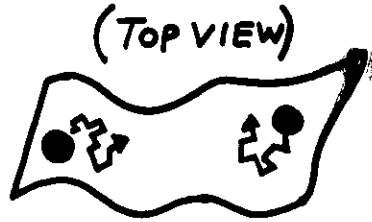

Polymer diffusion in 2D membrane

) Bare membrane flexible : repulsive undulation forces stabilize multilayers

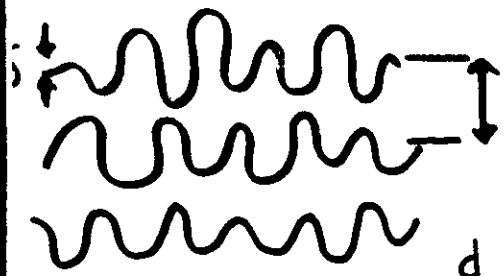

$d \gg \delta$

$d_{max} \simeq 420\,A \gg R_G$

Elastic Free Energy of Interface [Helfrich 73]

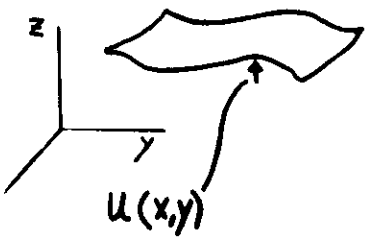

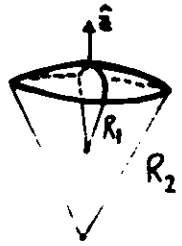

principle curvature radii: R_1, R_2

$$F_{(\text{unit area})} = \frac{k_c}{2}\left[C_1 + C_2 - C_0\right]^2 + \bar{k} C_1 C_2$$

Curvatures: $C_1 = 1/R_1 \approx \frac{\partial^2 u}{\partial x^2}$, $C_2 = 1/R_2 \approx \frac{\partial^2 u}{\partial y^2}$

$C_0 = 2/R_0$; R_0 = natural radius of curvature

monolayer interface asymmetry $\Rightarrow C_0 \neq 0$

1st term: deviations from C_0 costs bend energy k_c

monolayer tubule $C_0 = 0$, - deviations from a flat surface

2nd term: drop, (consider lamellar L_α phase only)

Thermal Fluctuations of Membranes

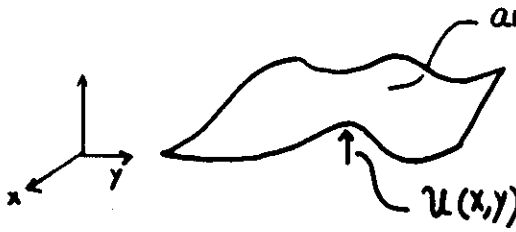

$$F = \frac{k_c}{2}\left(\frac{\partial^2 u}{\partial x^2} + \frac{\partial^2 u}{\partial y^2}\right)^2$$

$$\langle u^2 \rangle = \sum_q \langle |u_q|^2 \rangle \sim \frac{kT}{k_c} A$$ violent fluctuations

k_c = bending modulus

Helfrich (1978, Z. Naturforsch):

Fluctuating multilayers ⟶ long range repulsion

"Free" Membrane: "Confined" between walls:

$$\Delta F_{(\text{unit area})} = \alpha \cdot k_B T \left(\frac{k_B T}{k_c}\right) \frac{1}{L^2} \qquad \alpha = 0.23$$

- Long range, repulsive interaction (undulation forces)

Height fluctuations cut off by neighbors

$\langle u^2 \rangle \sim \frac{k_B T}{k_c} A$, when $\sqrt{\langle u^2 \rangle} \sim d$ collisions occurs

> defines a patch size A_p which will experience collision

$$A_p \simeq \frac{k_c}{k_B T} d^2$$

$$\frac{F_{entropy}}{Area} = (k_B T)\left(\frac{\#\ of\ collisions}{Area}\right) = \frac{k_B T}{A_p} \sim \frac{(k_B T)^2}{k_c d^2}$$

ther systems: Incommensurate - Commensurate transition
e.g. Br intercalated graphite: Moncton, Kortan, Birgeneau, Horn (Z. Phys.)

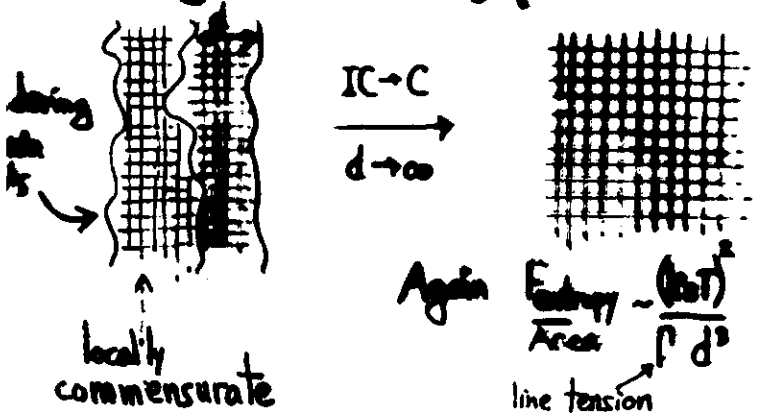

Again $\frac{E_{entropy}}{Area} \sim \frac{(k_B T)^2}{\Gamma d^3}$ (Villain, Re... J. de Phys...

Forces between Flat Sheets (Continuum limit)

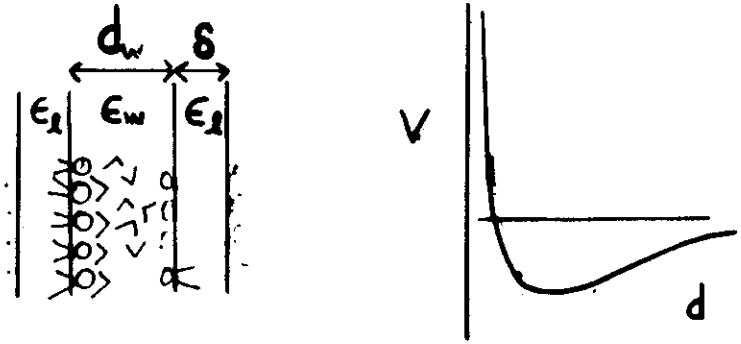

Neutral Membranes

1) **Long Range attraction (van der Waals)** [Lifshitz et al. (1959)]

$$\frac{F}{A} = -\frac{H}{12\pi}\left\{\frac{1}{(d_T-\delta)^2} + \frac{1}{(d_T+\delta)^2} - \frac{2}{d_T^2}\right\} = -.018\,kT\{\ \}$$

$\sim -1/(d_T-\delta)^2$, $d_T \approx \delta$

$\sim -1/d_T^4$, $d_T \gg \delta$

$$H = \left(\frac{\epsilon_w - \epsilon_l}{\epsilon_w + \epsilon_l}\right)^2 \cdot kT$$

[Israelachvili et al. (1973)]

2) **Short Range repulsion (hydration)** ←

$$\frac{F}{A} = A_h e^{-(d_T-\delta)/\lambda_h}$$

$A_h \sim 4\ kT/\text{Å}^2$

$\lambda_h \sim 2$ Å

[Marcelja, Radic, Rand (1976)]

Recall Interactions

A. Undulations (mutual repulsion of wandering sheets)

$$F_u/\text{Area} = \frac{0.23(k_B T)^2}{k_c\, d_o^2} \sim (0.12 \to 0.46)\, k_B T/d_o^2$$

B. van der Waals (attraction)

$$F_{v.d.W.}/\text{Area} \simeq -\frac{H}{12\pi}\left(\frac{1}{d_o^2} + \frac{1}{(d_o+2d_w)^2} - \frac{2}{(d_o+d_w)^2}\right)$$

$$\approx -(0.014 \to 0.002)\, k_B T/d_o^2$$

- Undulation Forces should dominate since $k_c \sim k_B T$ for these interfaces.

OIL (DODECANE) DILUTION OF LAMELLAR PHASE

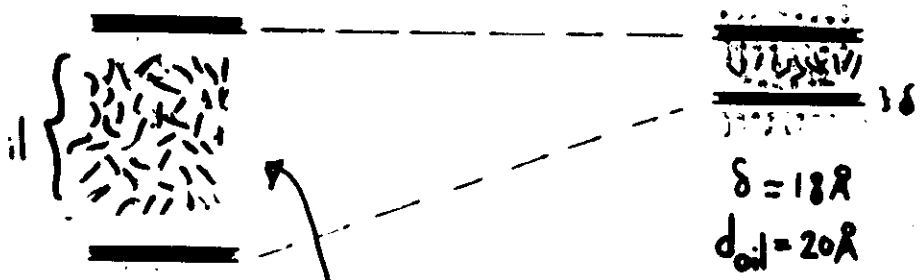

Undulation Interactions Stabilize Lamellar L$_\alpha$

First harmonic data

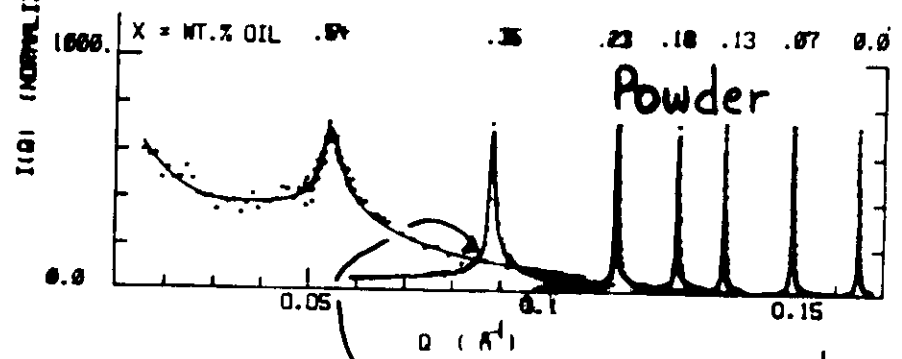

Tail scattering $I(q) \sim \frac{1}{(q-q_o)^{1-\eta_u}}$

Oriented:

$$Q_{peak} = \frac{2\pi}{d} = \frac{2\pi}{d_{oil}+\delta}$$

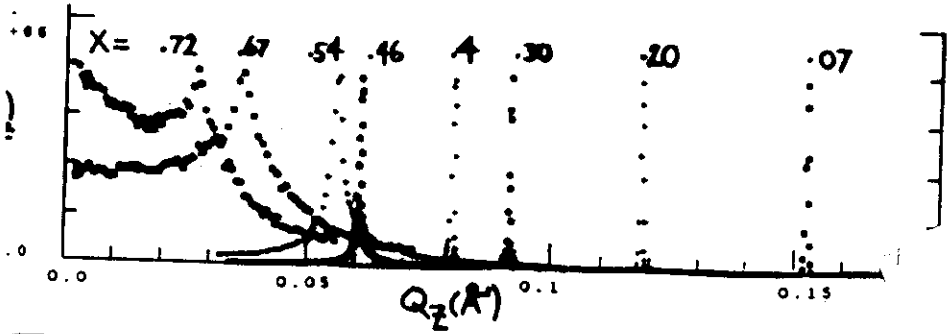

Experimental Results - Helfrich theory (undulation forces

$\eta_1 = 1.33\,(1-\delta/d)^2$ $\quad \delta$ = membrane thickness

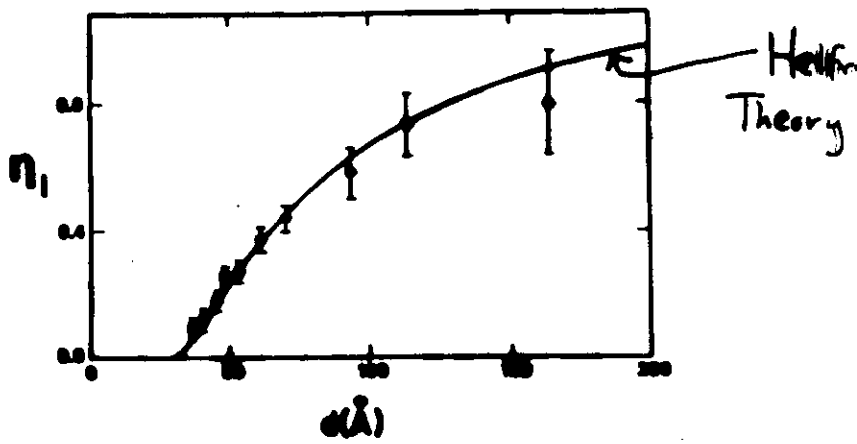

- η not a function of k_c ($\eta \sim \frac{1}{(Bk_c)^{1/2}}$ & $B \sim 1/k_c$)
- η is a simple universal function of (δ/d)

B: layer compressibility modulus

K_c: layer bending

papers: PRL; v57, 2718(1986); v62, 1134 (1989)
J. Phys. (Fr); v49, (1988), p.307

Peg 2000 Phase Diagram

R_g = 35Å

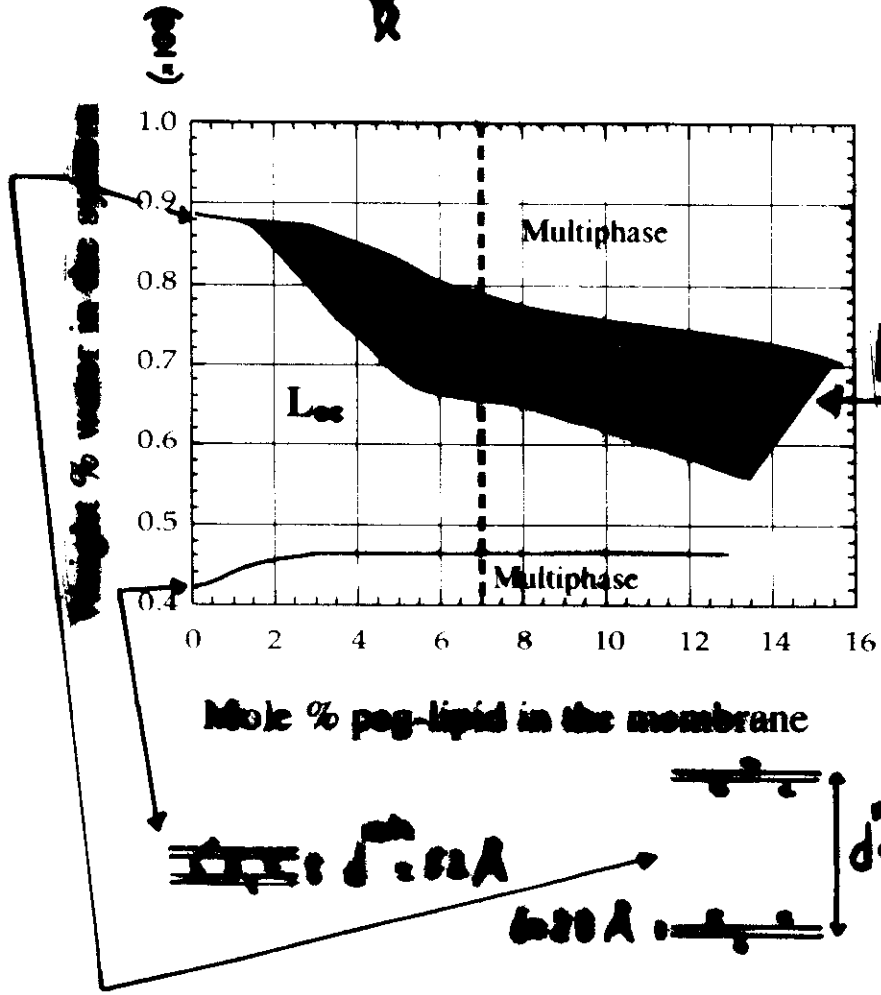

- New Phase: (Lyotropic Liquid Crystal) L_α, Gel

high water regime; lipid chains fluid (L_β, gels/fro chai

One-Dimensionally Ordered Lamellar Biogel

Less polymer is required for gelation as water content is increased: this is due to the underlying 1-D ordering (opposite behavior compared to disordered gels)

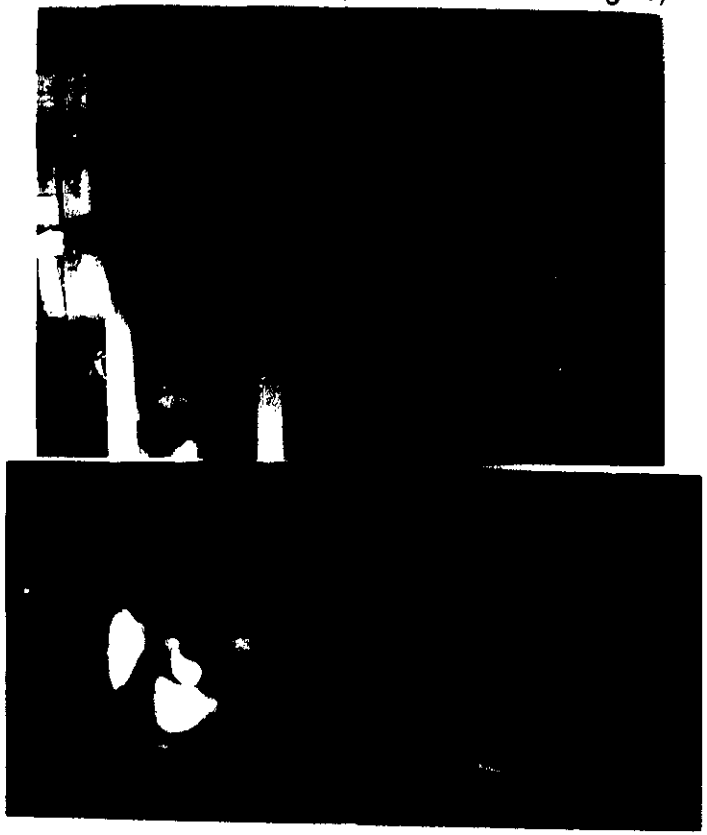

B. Liquid crystal defect structure (resulting from the one-dimensional ordering) is evident between crossed polarizers.
C. Elasticity is shown by the observation of stable non-spherical air bubbles.

α, Gel

Lamellar Biogels are Stabilized at High Water Concentrations

- This system is a one-dimensional ordered gel. Traditional polymer gels are disordered.
- A large gel regime below **monolayer coverage** is observed.

(The gel phase forms at $c \ll c^*$ concentrations of polymer as low as ≈ 0.2%w/w PEG 5000)

c*: 

≈[mushroom-brush transition]

(This suggests that the simple entanglement between layers for $c \approx c^*$ of the peg-lipid polymers can not be responsible for the gel.)

- i.e. gelation in mushroom regime away brush regime.

$c < c^*$ 

- How is the biogel formed? Look at larger scales.

Defect ($\pm\frac{1}{2}$ disclinations) Formation

oliferation of defects: "softening" of defect line tension

Defects ⟶ elastic behavior of $L_{\alpha,Gel}$

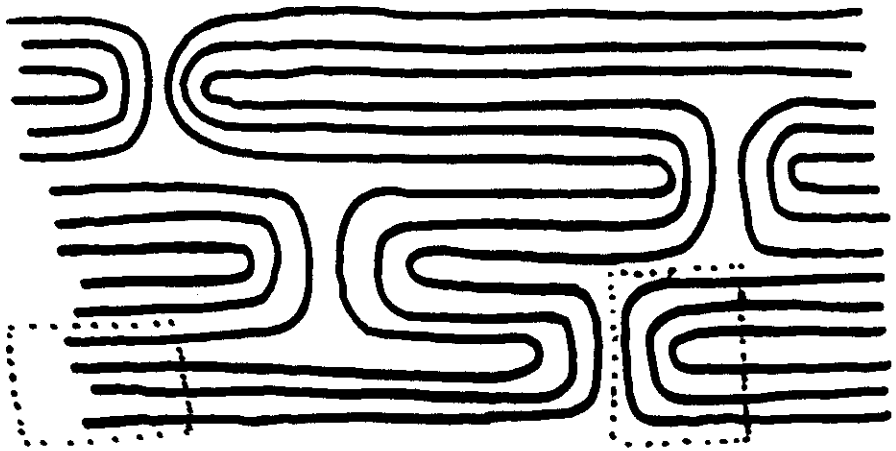

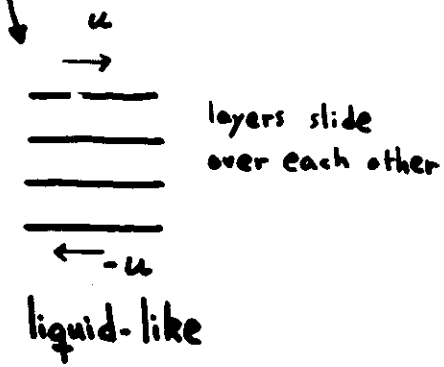

liquid-like

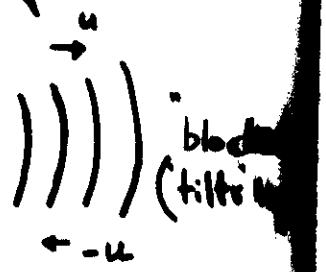

solid-like

$G'(\Phi^{PEG})$

$L_{\alpha,Gel}$ = visco-elastic

- Defects (regions of aggregation of PEG-L) can not be annealed

Control Mechanism of Gel Formation (Fluid Me